

Supporting Information

Capturing Ultrafast Energy Flow of a Heme Protein In Crowded Milieu

Shubhangi Majumdar, Ambika Prasad Kar, Jaydeep Basu, Pramit K Chowdhury*

Department of Chemistry, Indian Institute of Technology Delhi,

Hauz Khas, New Delhi 110016

* To whom correspondence should be addressed:

Email : pramitc@chemistry.iitd.ac.in

Tel : +911126591521

Experimental Section:

Details of Global Analyses

To analyze the complex transient absorption spectra (TAS), first, we fitted single wavelength decay profiles at the corresponding excited state absorption maxima to gain prior knowledge about the time constants (Figure 1E and F, SI Tables S1, S5-S9 and SI Figures S3). However, the time constants extracted from a single wavelength fit may represent a composite of multiple coinciding processes owing to overlapping features in TA spectra. Systematically fitting and analyzing each individual wavelength can be quite laborious and time-consuming. Therefore, the dynamical parameters are derived by fitting the complete set of TA spectra through global analysis.¹⁻³ The global analysis assumes that the data are completely separable spectrally and temporally, where the data matrix is represented as follows.

$$\Delta A_{exp}(\lambda, t) = S(\lambda) \cdot C(t) \quad (S1)$$

$S(\lambda)$ is representing transient absorption spectra as a function of wavelength in the form of ‘m’ by ‘k’ matrix and $C(t)$ is for the time-dependent one, denoted by the ‘k’ by ‘n’ matrix. Here, ‘m’ stands for wavelengths, ‘n’ as delay time points, and ‘k’ represents no. of distinct spectral components used to reproduce the spectra, assuming each component to have single exponential kinetics.¹⁻³

Then, singular value decomposition algorithm using glotaran software was applied to the data matrices (as mentioned above) based on the guess values (values of ‘k’) obtained from the single wavelength fitting, to obtain the timescales of global dynamics associated with the species as described below.¹⁻³ The variation of the amplitude of each time component spectrally over the entire wavelength range is obtained in the form of corresponding Decay-associated spectra (DAS) or Decay-associated difference spectra (DADS). For obtaining DAS, we generated $C_{guess}(t)$ and obtained $S_{fit}(\lambda)$ as shown below.

$$S = A(C^T C)^{-1} C^T \quad (S2)$$

$$[S_{fit}(\lambda) = S, \Delta A_{exp}(\lambda, t) = A \text{ and } C_{guess}(t) = C]$$

$$S = A \cdot C^+ \quad (S3)$$

Where C^+ is the Moore-Penrose pseudoinverse, denoted as $C^+ = (C^T C)^{-1} C^T$

The product of $S_{fit}(\lambda)$ and $C_{guess}(t)$ yields $\Delta A_{fit}(\lambda, t)$ (equation S6), subsequently, minimizing residuals [$\Delta A_{exp}(\lambda, t) - \Delta A_{fit}(\lambda, t)$], optimal $S_{fit}(\lambda)$ and time constants were obtained.³

$$\Delta A_{fit}(\lambda, t) = S \cdot C = A \cdot C^+ \cdot C \quad (S4)$$

The study by van Stokkum and coworkers¹ has provided a more comprehensive understanding of the mathematical and technological components of globally analyzing transient absorption spectra.

We did not blindly rely on software-generated data. Rather, to check the reliability of the components obtained from the global analyses, we re-used the globally obtained components to fit the single-wavelength decay traces over a wide range of wavelengths of the transient absorption spectra. Further, the average lifetimes calculated from the decay parameters probing at a particular wavelength (at 600 nm, which is the maximum of the ESA band in the wavelength range 570-700 nm, although the whole range has shown similar kinetics) show similar trends as function of crowder concentration as that obtained from global analyses. The decay kinetics at 600 nm have been shown already (Figures 5E, F and SI Figure S4, Tables S1).

References

- 1 I. H. M. Van Stokkum, D. S. Larsen and R. Van Grondelle, *Biochim. Biophys. Acta - Bioenerg.*, 2004, **1657**, 82-104.
- 2 J. Beckwith, C. A. Rumble and E. Vauthey, *Int. Rev. Phys. Chem.*, 2020, **39**, 135-216.
- 3 R. Hamburger, C. Rumble and E. R. Young, *J. Vis. Exp.*, 2024, **204**, e65519.

Photoreduction and oxidation of the protein

Multiple groups have documented the possibility of photoreduction and oxidation of heme iron under irradiation; however, the precise mechanism of such long-lasting photoproduct formation remains unknown.¹⁻⁶ While there was speculation of photo redox phenomena occurring upon exposure to UV irradiation, indicating that aromatic amino acid residues may serve as electron donors,² visible wavelength excitation have also been shown to give rise to the same effect. The axial ligands and amino acid residues in close proximity to the heme group are observed to play a vital part in this photoreduction.³⁻⁶ To investigate the formation of photoproducts, we compared the ground state absorption spectrum of ferric Cyt c before and after 1 hour of laser irradiation, with negligible change in the spectral signature (SI Figure S16A). However, chemically reducing the same irradiated sample has confirmed the presence of the fully reduced species from the red-shifted Soret band and prominently split Q-band. Further, we overlapped the differential ground state absorption spectra of ferric and ferrous Cyt c and transient absorption spectra of ferric at late time delay (20 ps), considering cooling

components are absent (SI Figure S16B). From the ratio of absorbances, the yield of photo-reduced Cyt *c* was calculated as mentioned elsewhere⁶ and found to be 0.0012 upon excitation by 400 nm laser, which is much less as compared to that reported in literature. The reason for such reduced photoreduction may lie in the fact that all transient absorption experiments with the ferric samples have been carried out under normal conditions wherein the high concentration of dissolved oxygen in phosphate buffer suppressed photoreduction.⁵ To confirm our observation further, we carried out transient absorption experiments of ferric Cyt *c* in buffer and 200 g/L of synthetic crowders (Dextran 40, 70, Ficoll 70, and PEG 8) after purging oxygen into each sample before recording spectra. The results obtained in both ambient and aerobic conditions show appreciable overlap with each other (SI Figures S17). Similarly, while investigating the possibility of photo-oxidation of ferrous Cyt *c*, negligible changes observed in the ground state absorption spectra of ferrous form before and after laser irradiation reduce the possibility of photo-oxidation (Figure S18A), which is further confirmed by the significant differences observed in spectral nature near the Q-band and shift in Soret band upon overlapping with the ground state absorption spectra of ferric Cyt *c* before laser exposure (black line) to the ferrous one after exposure (blue line). The extremely low yield⁶ of 0.00034 calculated by comparing transient absorption spectra of ferrous Cyt *c* at 20 ps (assuming cooling is completed at a longer time delay) and differential ground state absorption spectra of ferric and ferrous Cyt *c*, extensively justifies the least probability of photooxidation of ferrous Cyt *c* (Figure S18B).

Interestingly, the pump laser intensity has been shown to have a direct impact on the photoreduction process.^{5,6} We conducted a power-dependent measurement of both the ferric and ferrous forms in buffer, where the ΔA at 530 nm (ground state bleach signal) vs. increasing pump power shows non-linearity beyond 0.6-0.7 mW (SI Figure S19A and S20A), while our working pump power lies within the linear limit (0.5 ± 0.03 mW). Increased laser intensity has brought about a gradual longer decay when probed at 600 nm for ferric (SI Figure S19B), and at 575 nm for ferrous (Figure 20B), not decaying within the limited time scale of our delay stage (~ 8 ns). In addition to the four components, a tiny infinite component had to be included in order to obtain the most accurate fit when pumping beyond 0.6 mW. The magnitudes of all five decay components have been tabulated, showing that the "Inf" component stays very low (< 0.01%) throughout the range of 0.3-0.5 mW but steadily increases to 2% at around 1 mW for ferric and ~3% at 0.8 mW of pump power for ferrous (SI Table S14, SI Table S15). Hence, it allows us to assign the "Inf" component as the photo redox

conversion timescale.^{1,6} Since the amplitude of this photo redox conversion timescale is very low (~ 0.0001) and the decay time is beyond instrument limitation (> 8 ns) at our working pump power, 0.5 mW, showing very little possibility of photoreduction or photooxidation of the species, we have carefully excluded this component from our discussion.

References

- 1 C. Consani, O. Bräm, F. Van Mourik, A. Cannizzo and M. Chergui, *Chem. Phys.*, 2012, **396**, 108-115.
- 2 T. Masuda, A. Minemura, K. Yamauchi and M. Kondo, *J. Radiat. Res.*, 1980, **21**, 149.
- 3 W. P. Vorkink and M. A. Cusanovich, *Photochem. Photobiol.*, 1973, **19**, 205.
- 4 C. Bartocci, A. Maldotti and O. Traverso, *Inorg. Chim. Acta*, 1985, **107**, 5.
- 5 Y. Gu, P. Li, J. T. Sage and P. M. Champion, *J. Am. Chem. Soc.*, 1993, **115**, 4993.
- 6 D. Lowenich, K. Kleinermanns, V. Karunakaran and S. A. Kovalenko, *Photochem. Photobiol.*, 2008, **84**, 193.

Table S1: Fitting parameters obtained from decay kinetics of ferric Cyt *c*, being probed at 600 nm, in the presence of crowders as a function of their increasing concentration (Independent experiments with ~ 10 % error).

PEG 8	a ₁	τ ₁ (ps)	a ₂	τ ₂ (ps)	a ₃	τ ₃ (ps)	a ₄	τ ₄ (ps)
0	0.510	0.120	0.0700	0.350	0.250	3.65	0.170	6.22
50	0.510	0.130	0.0600	0.910	0.340	4.35	0.0800	385
100	0.520	0.140	0.0800	0.810	0.350	5.29	0.0500	650.
150	0.500	0.140	0.0550	0.850	0.400	4.21	0.0450	820.
200	0.480	0.150	0.0100	0.950	0.460	2.82	0.0400	901

Dextran 40	a ₁	τ ₁ (ps)	a ₂	τ ₂ (ps)	a ₃	τ ₃ (ps)	a ₄	τ ₄ (ps)
0	0.510	0.120	0.0700	0.350	0.250	3.65	0.170	6.22
50	0.440	0.110	0.0500	0.440	0.440	3.70	0.0700	16.0
100	0.440	0.110	0.0500	0.530	0.470	4.30	0.0400	21.0
150	0.400	0.150	0.0300	0.550	0.550	5.20	0.0200	53.0
200	0.400	0.150	0.0200	1.30	0.570	5.34	0.0100	93.0

Ficoll 70	a ₁	τ ₁ (ps)	a ₂	τ ₂ (ps)	a ₃	τ ₃ (ps)	a ₄	τ ₄ (ps)
0	0.510	0.120	0.0700	0.350	0.250	3.65	0.170	6.22
50	0.520	0.130	0.0700	0.320	0.320	5.40	0.0800	49.0
100	0.480	0.130	0.0700	0.620	0.410	5.50	0.0400	86.0
150	0.470	0.150	0.0500	1.50	0.450	5.21	0.0300	127
200	0.450	0.130	0.0600	0.880	0.440	3.70	0.0500	36.0

Dextran 70	a ₁	τ ₁ (ps)	a ₂	τ ₂ (ps)	a ₃	τ ₃ (ps)	a ₄	τ ₄ (ps)
0	0.510	0.120	0.0700	0.350	0.250	3.65	0.170	6.22
50	0.490	0.120	0.0900	0.750	0.310	4.64	0.110	10.0
100	0.510	0.140	0.0300	0.800	0.360	4.61	0.100	13.5
150	0.520	0.140	0.0200	0.850	0.390	5.65	0.0700	51.0
200	0.500	0.150	0.0500	0.950	0.340	3.95	0.110	25.0

BSA	a₁	τ₁(ps)	a₂	τ₂(ps)	a₃	τ₃(ps)	a₄	τ₄(ps)
0	0.510	0.120	0.0700	0.350	0.250	3.65	0.170	6.22
25	0.440	0.150	0.300	2.90	0.160	11.3	0.100	220.
50	0.220	0.230	0.530	1.45	0.180	15.0	0.0900	350.
75	0.240	0.350	0.490	3.34	0.190	22.3	0.0600	725
100	0.270	0.500	0.470	3.73	0.200	49.9	0.0600	968
125	0.280	0.150	0.290	1.02	0.340	5.14	0.0900	125
150	0.390	0.130	0.200	1.11	0.300	4.48	0.110	49.0

β-LG	a₁	τ₁(ps)	a₂	τ₂(ps)	a₃	τ₃(ps)	a₄	τ₄(ps)
0	0.510	0.120	0.0700	0.350	0.250	3.65	0.170	6.22
25	0.490	0.120	0.230	0.380	0.160	2.90	0.130	108
50	0.480	0.130	0.270	0.420	0.180	3.23	0.120	130.
75	0.490	0.150	0.240	0.480	0.190	3.16	0.0800	190.
100	0.470	0.180	0.270	0.560	0.200	3.73	0.0600	360.
125	0.320	0.150	0.290	0.440	0.310	4.08	0.0800	96.0
150	0.440	0.140	0.360	0.390	0.300	4.12	0.100	65.0

[Glucose] (g/L)	a₁	τ₁(ps)	a₂	τ₂(ps)	a₃	τ₃(ps)	a₄	τ₄(ps)
0	0.510	0.120	0.0700	0.350	0.250	3.65	0.170	6.22
50	0.500	0.130	0.0600	0.400	0.280	4.10	0.160	8.50
100	0.490	0.150	0.0600	0.460	0.310	3.70	0.140	13.0
150	0.500	0.140	0.0500	0.570	0.360	3.90	0.0900	81.0
200	0.480	0.130	0.0500	0.610	0.410	3.50	0.0600	137

[Sucrose] (g/L)	a₁	τ₁(ps)	a₂	τ₂(ps)	a₃	τ₃(ps)	a₄	τ₄(ps)
0	0.510	0.120	0.0700	0.350	0.250	3.65	0.170	6.22
50	0.500	0.140	0.0600	0.470	0.290	2.80	0.150	10.0
100	0.510	0.130	0.0600	0.500	0.300	3.30	0.130	18.0
150	0.520	0.150	0.0700	0.310	0.270	3.10	0.140	14.0
200	0.510	0.120	0.0800	0.250	0.260	2.90	0.150	11.0

[Ethylene Glycol] (g/L)	a₁	τ₁(ps)	a₂	τ₂(ps)	a₃	τ₃(ps)	a₄	τ₄(ps)
0	0.510	0.120	0.0700	0.350	0.250	3.65	0.170	6.22
50	0.510	0.130	0.0700	0.370	0.270	3.50	0.150	9.00
100	0.500	0.120	0.0600	0.420	0.310	3.70	0.130	15.0
150	0.490	0.150	0.0600	0.490	0.330	3.60	0.120	18.0
200	0.480	0.170	0.0500	0.540	0.370	4.10	0.100	23.0

Table S2: The principal components obtained from singular value decomposition (SVD) of the transient absorption data for ferric Cyt *c* in buffer and in the presence of synthetic polymeric crowders (Independent experiments with ~ 10 % error).

Crowder (g/L)	Dextran 40				PEG 8			
	τ_1 (ps)	τ_2 (ps)	τ_3 (ps)	τ_4 (ps)	τ_1 (ps)	τ_2 (ps)	τ_3 (ps)	τ_4 (ps)
0	0.120±0.010	0.330±0.110	5.00±1.25	9.18±1.01	0.120±0.010	0.330±0.110	5.00±1.25	9.18±1.01
50	0.130±0.020	0.500±0.200	5.50±1.22	20.0±1.00	0.130±0.020	0.560±0.310	6.67±1.37	400.±1.2
100	0.170±0.030	0.670±0.130	5.00±1.21	25.0±1.00	0.160±0.030	0.830±0.410	8.50±1.14	622±6.5
150	0.180±0.040	1.00±0.03	5.00±1.25	66.6±1.0	0.180±0.040	1.00±0.36	3.80±0.93	800.±9.7
200	0.220±0.060	1.61±0.27	4.64±1.08	95.9±2.3	0.200±0.050	2.10±0.50	5.00±1.02	1000±11

Crowder (g/L)	Dextran 70				Ficoll 70			
	τ_1 (ps)	τ_2 (ps)	τ_3 (ps)	τ_4 (ps)	τ_1 (ps)	τ_2 (ps)	τ_3 (ps)	τ_4 (ps)
0	0.120±0.010	0.330±0.110	5.00±1.30	9.18±1.01	0.120±0.010	0.330±0.110	5.00±1.25	9.18±1.01
50	0.120±0.010	0.667±0.130	3.08±0.25	10.6±1.2	0.150±0.020	0.690±0.100	4.42±0.73	69.4±1.3
100	0.130±0.020	0.830±0.420	2.73±0.38	14.4±3.7	0.180±0.050	0.960±0.270	4.47±0.83	100.±1.0
150	0.150±0.030	0.840±0.400	3.70±0.27	46.5±1.4	0.190±0.060	1.12±0.33	4.60±0.56	111±1.0
200	0.130±0.040	0.680±0.230	3.73±0.51	20.0±1.0	0.110±0.060	0.550±0.400	3.78±0.23	46.7±1.4

Table S3: The principal components obtained from singular value decomposition (SVD) of the transient absorption data for ferrous Cyt *c* in buffer and in the presence of synthetic polymeric crowders (Independent experiments with ~ 10 % error).

Crowder (g/L)	Dextran 40				PEG 8			
	τ_1 (ps)	τ_2 (ps)	τ_3 (ps)	τ_4 (ps)	τ_1 (ps)	τ_2 (ps)	τ_3 (ps)	τ_4 (ps)
0	0.220±0.410	0.560±0.070	2.77±0.16	7.20±1.06	0.220±0.410	0.560±0.070	2.77±0.16	7.20±1.06
50	0.250±0.080	0.910±0.070	3.64±0.37	8.88±1.14	0.260±0.090	1.01±0.11	4.16±0.10	12.4±0.6
100	0.270±0.100	1.40±0.09	4.60±0.56	12.6±1.1	0.260±0.090	0.720±0.140	4.27±0.82	14.6±1.1
150	0.290±0.130	1.48±0.14	5.31±0.67	13.2±1.1	0.290±0.050	0.690±0.130	3.96±0.78	22.7±0.6
200	0.310±0.140	1.54±0.29	5.03±0.59	14.7±1.1	0.280±0.120	0.650±0.130	4.79±0.77	24.2±1.1

Crowder (g/L)	Dextran 70				Ficoll 70			
	τ_1 (ps)	τ_2 (ps)	τ_3 (ps)	τ_4 (ps)	τ_1 (ps)	τ_2 (ps)	τ_3 (ps)	τ_4 (ps)
0	0.220±0.410	0.560±0.070	2.77±0.16	7.20±1.06	0.220±0.410	0.560±0.070	2.77±0.16	7.20±1.06
50	0.230±0.050	0.650±0.070	3.84±0.36	13.7±0.6	0.210±0.060	0.790±0.080	3.04±0.53	8.90±0.91
100	0.250±0.080	0.950±0.130	4.19±0.71	20.6±0.5	0.260±0.090	1.80±0.33	4.47±0.33	10.1±1.1
150	0.260±0.050	0.640±0.320	4.32±0.53	24.7±1.1	0.150±0.090	0.300±0.130	1.35±0.26	5.41±1.4
200	0.260±0.060	0.530±0.260	4.20±0.51	20.2±1.1	0.180±0.040	0.280±0.110	1.15±0.76	5.11±1.6

Table S4: Variation in the blue shift of ESA band \sim 575- 600 nm with time delay and comparison of the amplitudes of cooling components calculated both from the spectra and fitting parameters of decay kinetics at corresponding maxima, 600 and 575 nm of ferric and ferrous Cyt c respectively in buffer and presence of synthetic crowders.

[In the second column (shift in λ), we have tabulated the extent of the blue shift in wavelength of the ESA band with an increasing time delay of both ferric and ferrous forms in buffer and in the presence of crowders as a function of their concentration, the third column (Time delay) represents the time delay till which blue shift is persistent, while the third column ($a_{cooling}$) compares the amplitude of cooling calculated from the transient absorption spectra with that of ' $a_1 + a_2$ ', which is the amplitude of cooling calculated from the combined amplitudes of τ_1 and τ_2 obtained from the exponential fitting of ESA maxima. ($\Delta A_{time\ zero} = \Delta A$ at initial time delay from which ESA starts decaying, $\Delta A_{no\ shift} = \Delta A$ at that time delay from which the blue shift and narrowing of the band are ended).]

PEG 8 (g/L)	Ferric		$a_{cooling} =$		Ferrous		$a_{cooling} =$	
	Shift in λ (nm)	Time delay (ps)	$1 - \frac{\Delta A_{no\ shift}}{\Delta A_{time\ zero}}$	$a_1 + a_2$ at 600 nm	Shift in λ (nm)	Time delay (ps)	$1 - \frac{\Delta A_{no\ shift}}{\Delta A_{time\ zero}}$	$a_1 + a_2$ at 575 nm
0	12.0	5.00	0.600	0.580	5.0	6.00	0.570	0.570
50	15.0	10.0	0.570	0.570	15.0	6.00	0.620	0.600
100	17.0	10.0	0.580	0.600	18.0	7.00	0.570	0.570
150	22.0	10.0	0.546	0.550	13.0	7.00	0.590	0.580
200	19.0	10.0	0.500	0.490	17.0	6.00	0.560	0.550

Dextran 40 (g/L)	Ferric		$a_{cooling} =$		Ferrous		$a_{cooling} =$	
	Shift in λ (nm)	Time delay (ps)	$1 - \frac{\Delta A_{no\ shift}}{\Delta A_{time\ zero}}$	$a_1 + a_2$ at 600 nm	Shift in λ (nm)	Time delay (ps)	$1 - \frac{\Delta A_{no\ shift}}{\Delta A_{time\ zero}}$	$a_1 + a_2$ at 575 nm
0	12.0	5.00	0.600	0.580	5.00	6.00	0.570	0.570
50	11.0	6.00	0.496	0.490	15.0	6.00	0.575	0.590
100	10.0	7.00	0.496	0.490	7.0	7.00	0.610	0.600
150	9.00	7.00	0.433	0.430	9.00	5.00	0.585	0.590
200	10.0	7.00	0.440	0.420	9.00	6.00	0.533	0.540

Ficoll 70	Ferric		$a_{cooling} =$	Ferrous		$a_{cooling} =$		
(g/L)	Shift in λ (nm)	Time delay (ps)	$1 - \frac{\Delta A_{no shift}}{\Delta A_{time zero}}$	$a_1 + a_2$ at 600 nm	Shift in λ (nm)	Time delay (ps)	$1 - \frac{\Delta A_{no shift}}{\Delta A_{time zero}}$	$a_1 + a_2$ at 575 nm
0	12.0	5.00	0.600	0.580	5.00	6.00	0.570	0.570
50	25.0	4.00	0.610	0.590	11.0	8.00	0.616	0.620
100	18.0	6.00	0.570	0.550	13.0	6.00	0.610	0.620
150	18.0	7.00	0.530	0.520	9.00	8.00	0.600	0.630
200	15.0	5.00	0.500	0.510	10.0	9.00	0.610	0.630

Dextran 70	Ferric		$a_{cooling} =$	Ferrous		$a_{cooling} =$		
(g/L)	Shift in λ (nm)	Time delay (ps)	$1 - \frac{\Delta A_{no shift}}{\Delta A_{time zero}}$	$a_1 + a_2$ at 600 nm	Shift in λ (nm)	Time delay (ps)	$1 - \frac{\Delta A_{no shift}}{\Delta A_{time zero}}$	$a_1 + a_2$ at 575 nm
0	12.0	5.00	0.600	0.580	5.00	6.00	0.570	0.570
50	18.0	5.00	0.590	0.580	22.0	6.00	0.570	0.580
100	20.0	5.00	0.550	0.540	18.0	7.00	0.530	0.520
150	26.0	5.00	0.570	0.540	18.0	6.00	0.480	0.490
200	18.0	5.00	0.560	0.550	23.0	6.50	0.525	0.510

Table S5: Fitting parameters obtained from decay kinetics of ferric Cyt *c*, being probed at 550 nm, in the presence of crowders as a function of their increasing concentration (Independent experiments with ~ 10 % error).

[Ficoll 70] (g/L)	(-) a_1	τ_1 (ps)	(-) a_2	τ_2 (ps)	(-) a_3	τ_3 (ps)	(-) a_4	τ_4 (ps)
0	0.490	0.120	0.0500	0.510	0.320	3.22	0.140	7.18
50	0.500	0.120	0.0600	0.350	0.370	6.77	0.0700	44.0
100	0.500	0.130	0.0700	0.490	0.390	6.86	0.0400	76.0
150	0.480	0.140	0.0500	0.780	0.450	6.96	0.0300	115
200	0.450	0.140	0.0600	0.730	0.440	4.04	0.0500	31.0

Table S6: Fitting parameters obtained from decay kinetics of ferric Cyt *c*, being probed at 435 nm, in the presence of crowders as a function of their increasing concentration (Independent experiments with ~ 10 % error).

[PEG 8] (g/L)	a_1	τ_1 (ps)	a_2	τ_2 (ps)	a_3	τ_3 (ps)
0	0.520	0.150	0.270	0.360	0.210	3.50
50	0.410	0.160	0.150	0.510	0.440	80.0
100	0.410	0.140	0.130	0.660	0.460	92.0
150	0.360	0.150	0.140	0.750	0.490	97.0
200	0.410	0.170	0.0800	0.830	0.510	105

[Dextran 40] (g/L)	a_1	τ_1 (ps)	a_2	τ_2 (ps)	a_3	τ_3 (ps)
0	0.520	0.150	0.270	0.360	0.210	3.50
50	0.450	0.150	0.250	0.360	0.200	3.98

100	0.460	0.150	0.150	0.390	0.390	4.22
150	0.380	0.150	0.100	0.440	0.520	4.86
200	0.350	0.140	0.0700	0.790	0.580	5.29

[Ficoll 70] (g/L)	a₁	τ₁ (ps)	a₂	τ₂ (ps)	a₃	τ₃ (ps)
0	0.520	0.150	0.270	0.360	0.210	3.50
50	0.410	0.140	0.150	0.450	0.440	12.0
100	0.410	0.130	0.130	0.750	0.460	15.0
150	0.360	0.150	0.140	0.900	0.490	16.0
200	0.420	0.140	0.0800	0.600	0.500	7.30

[Dextran 70] (g/L)	a₁	τ₁ (ps)	a₂	τ₂ (ps)	a₃	τ₃ (ps)
0	0.520	0.150	0.270	0.360	0.210	3.50
50	0.410	0.130	0.180	0.500	0.410	6.50
100	0.410	0.140	0.130	0.710	0.460	7.80
150	0.350	0.150	0.190	0.870	0.460	13.0
200	0.460	0.120	0.0900	0.910	0.450	10.0

[BSA] (g/L)	a₁	τ₁ (ps)	a₂	τ₂ (ps)	a₃	τ₃ (ps)
0	0.520	0.150	0.270	0.360	0.210	3.50
25	0.450	0.180	0.280	1.50	0.290	92.0

50	0.430	0.250	0.240	2.10	0.310	129
75	0.430	0.310	0.240	2.90	0.330	200.
100	0.400	0.420	0.240	3.40	0.360	275
125	0.390	0.230	0.190	1.30	0.420	50.0
150	0.400	0.160	0.160	1.00	0.440	17.0

[β -LG] (g/L)	a_1	τ_1 (ps)	a_2	τ_2 (ps)	a_3	τ_3 (ps)
0	0.520	0.150	0.270	0.360	0.210	3.50
25	0.490	0.130	0.240	0.320	0.270	50.0
50	0.500	0.140	0.200	0.370	0.300	55.0
75	0.490	0.150	0.220	0.430	0.290	61.0
100	0.490	0.130	0.240	0.470	0.270	90.0
125	0.430	0.130	0.180	0.330	0.390	25.0
150	0.430	0.120	0.170	0.290	0.400	21.0

[Glucose] (g/L)	a_1	τ_1 (ps)	a_2	τ_2 (ps)	a_3	τ_3 (ps)
0	0.520	0.150	0.270	0.360	0.210	3.50
50	0.500	0.160	0.110	0.390	0.390	6.10
100	0.490	0.150	0.0800	0.430	0.430	6.80
150	0.470	0.140	0.0800	0.490	0.450	20.0
200	0.480	0.130	0.0500	0.450	0.470	23.0

[Sucrose] (g/L)	a₁	τ₁ (ps)	a₂	τ₂ (ps)	a₃	τ₃ (ps)
0	0.520	0.150	0.270	0.360	0.210	3.50
50	0.500	0.130	0.190	0.410	0.310	5.40
100	0.490	0.130	0.140	0.450	0.370	7.80
150	0.490	0.150	0.100	0.340	0.410	4.60
200	0.500	0.130	0.0900	0.290	0.410	5.50

[Ethylene Glycol] (g/L)	a₁	τ₁ (ps)	a₂	τ₂ (ps)	a₃	τ₃ (ps)
0	0.520	0.150	0.270	0.360	0.210	3.50
50	0.500	0.160	0.150	0.370	0.350	5.40
100	0.500	0.140	0.110	0.390	0.390	6.90
150	0.480	0.170	0.0900	0.420	0.430	7.30
200	0.490	0.180	0.0500	0.450	0.460	8.10

Table S7: Fitting parameters obtained from decay kinetics of ferrous Cyt *c*, being probed at 575 nm, in the presence of crowders as a function of their increasing concentration (Independent experiments with ~ 10 % error).

[PEG 8] (g/L)	a ₁	τ ₁ (ps)	a ₂	τ ₂ (ps)	a ₃	τ ₃ (ps)	a ₄	τ ₄ (ps)
0	0.470	0.180	0.100	0.520	0.230	2.10	0.200	7.90
50	0.510	0.230	0.090	0.870	0.300	3.90	0.100	10.6
100	0.520	0.260	0.050	0.710	0.340	4.20	0.0900	13.1
150	0.490	0.290	0.060	0.590	0.390	3.80	0.0600	19.0
200	0.520	0.270	0.030	0.510	0.420	4.55	0.0300	21.0

[Dextran 40] (g/L)	a ₁	τ ₁ (ps)	a ₂	τ ₂ (ps)	a ₃	τ ₃ (ps)	a ₄	τ ₄ (ps)
0	0.470	0.180	0.100	0.520	0.230	2.10	0.200	7.90
50	0.500	0.240	0.0900	0.870	0.280	3.40	0.130	8.70
100	0.500	0.260	0.100	1.30	0.300	4.80	0.100	11.5
150	0.510	0.290	0.0800	1.60	0.320	5.80	0.090	14.0
200	0.480	0.300	0.0600	1.65	0.390	4.95	0.0700	17.0

[Ficoll 70] (g/L)	a ₁	τ ₁ (ps)	a ₂	τ ₂ (ps)	a ₃	τ ₃ (ps)	a ₄	τ ₄ (ps)
0	0.470	0.180	0.100	0.520	0.230	2.10	0.200	7.90
50	0.540	0.230	0.080	0.780	0.250	3.00	0.110	10.5
100	0.550	0.260	0.070	1.10	0.290	4.30	0.0900	11.8
150	0.580	0.190	0.050	0.480	0.300	1.88	0.0700	6.00
200	0.570	0.140	0.060	0.300	0.270	1.50	0.100	5.50

[Dextran 70] (g/L)	a ₁	τ ₁ (ps)	a ₂	τ ₂ (ps)	a ₃	τ ₃ (ps)	a ₄	τ ₄ (ps)
0	0.470	0.180	0.100	0.520	0.230	2.10	0.200	7.90
50	0.510	0.210	0.070	0.590	0.270	3.50	0.150	13.7
100	0.450	0.240	0.070	0.910	0.370	4.00	0.110	22.0
150	0.440	0.270	0.050	0.610	0.450	4.50	0.0600	27.0
200	0.450	0.260	0.060	0.450	0.410	3.90	0.0800	19.0

[BSA] (g/L)	a ₁	τ ₁ (ps)	a ₂	τ ₂ (ps)	a ₃	τ ₃ (ps)	a ₄	τ ₄ (ps)
0	0.470	0.180	0.100	0.520	0.230	2.10	0.200	7.90
25	0.440	0.210	0.0900	0.570	0.290	4.60	0.170	97.0
50	0.430	0.240	0.0900	0.620	0.340	4.70	0.140	423
75	0.410	0.290	0.0800	0.670	0.380	4.50	0.130	495
100	0.380	0.330	0.0900	0.730	0.420	5.80	0.110	731
125	0.400	0.270	0.0900	0.520	0.360	4.30	0.150	302
150	0.400	0.220	0.0900	0.490	0.330	4.00	0.180	75.0

[β-LG] (g/L)	a ₁	τ ₁ (ps)	a ₂	τ ₂ (ps)	a ₃	τ ₃ (ps)	a ₄	τ ₄ (ps)
0	0.470	0.180	0.100	0.520	0.230	2.10	0.200	7.90
25	0.440	0.200	0.0800	0.560	0.310	5.10	0.170	25.0
50	0.430	0.220	0.0900	0.600	0.330	5.30	0.150	77.0
75	0.420	0.250	0.100	0.610	0.350	5.40	0.130	100.
100	0.430	0.300	0.0900	0.590	0.340	5.20	0.140	88.0
125	0.450	0.280	0.0900	0.550	0.300	4.90	0.160	65.0
150	0.450	0.240	0.0900	0.540	0.290	4.80	0.170	49.0

[Glucose] (g/L)	a ₁	τ ₁ (ps)	a ₂	τ ₂ (ps)	a ₃	τ ₃ (ps)	a ₄	τ ₄ (ps)
0	0.470	0.180	0.100	0.520	0.230	2.10	0.200	7.90
50	0.480	0.190	0.0700	0.920	0.300	4.50	0.150	9.30
100	0.500	0.250	0.0800	0.730	0.290	4.60	0.130	11.0
150	0.490	0.260	0.0800	0.880	0.320	5.30	0.110	13.0
200	0.500	0.280	0.0600	0.570	0.350	4.90	0.0900	17.0

[Sucrose] (g/L)	a ₁	τ ₁ (ps)	a ₂	τ ₂ (ps)	a ₃	τ ₃ (ps)	a ₄	τ ₄ (ps)
0	0.470	0.180	0.100	0.520	0.230	2.10	0.200	7.90
50	0.490	0.250	0.090	0.610	0.250	3.50	0.170	13.0
100	0.490	0.290	0.080	0.770	0.290	5.10	0.140	24.0
150	0.480	0.260	0.090	0.630	0.280	4.20	0.150	16.0
200	0.490	0.250	0.100	0.510	0.250	4.50	0.160	14.0

[Ethylene Glycol] (g/L)	a ₁	τ ₁ (ps)	a ₂	τ ₂ (ps)	a ₃	τ ₃ (ps)	a ₄	τ ₄ (ps)
0	0.470	0.180	0.100	0.520	0.230	2.10	0.200	7.90
50	0.490	0.240	0.0900	0.550	0.250	4.50	0.180	8.50
100	0.510	0.270	0.0700	0.730	0.260	5.30	0.160	9.60
150	0.510	0.300	0.0700	0.820	0.280	5.80	0.140	11.0
200	0.500	0.360	0.0600	1.20	0.320	3.80	0.120	14.0

Table S8: Fitting parameters obtained from decay kinetics of ferrous Cyt *c*, being probed at 550 nm, in the presence of crowders as a function of their increasing concentration (Independent experiments with ~ 10 % error).

[Ficoll 70] (g/L)	(-) a_1	τ_1 (ps)	(-) a_2	τ_2 (ps)	(-) a_3	τ_3 (ps)	(-) a_4	τ_4 (ps)
0	0.480	0.150	0.110	0.590	0.220	2.40	0.190	8.30
50	0.470	0.210	0.0500	0.760	0.370	3.10	0.0700	10.0
100	0.460	0.260	0.0500	0.970	0.390	4.00	0.0400	12.0
150	0.460	0.180	0.0400	0.430	0.450	1.98	0.0300	6.30
200	0.450	0.150	0.0400	0.250	0.440	1.60	0.0500	5.90

Table S9: Fitting parameters obtained from decay kinetics of ferrous Cyt *c*, being probed at 430 nm, in the presence of crowders as a function of their increasing concentration (Independent experiments with ~ 10 % error).

[PEG 8] (g/L)	a_1	τ_1 (ps)	a_2	τ_2 (ps)	a_3	τ_3 (ps)
0	0.480	0.200	0.120	0.680	0.400	4.90
50	0.490	0.230	0.100	0.700	0.410	5.60
100	0.500	0.270	0.0700	0.750	0.430	6.20
150	0.500	0.290	0.0500	0.710	0.450	6.80
200	0.510	0.310	0.0400	0.650	0.450	8.70

[Dextran 40] (g/L)	a ₁	τ ₁ (ps)	a ₂	τ ₂ (ps)	a ₃	τ ₃ (ps)
0	0.480	0.200	0.120	0.680	0.400	4.90
50	0.490	0.230	0.100	0.750	0.410	5.00
100	0.500	0.260	0.100	1.40	0.400	6.50
150	0.510	0.270	0.0800	1.70	0.410	7.60
200	0.490	0.290	0.0800	1.90	0.430	7.90

[Ficoll 70] (g/L)	a ₁	τ ₁ (ps)	a ₂	τ ₂ (ps)	a ₃	τ ₃ (ps)
0	0.480	0.200	0.120	0.680	0.400	4.90
50	0.500	0.240	0.140	0.710	0.360	5.30
100	0.510	0.250	0.110	0.750	0.380	6.10
150	0.530	0.210	0.100	0.780	0.370	2.80
200	0.550	0.170	0.0800	0.800	0.370	2.60

[Dextran 70] (g/L)	a ₁	τ ₁ (ps)	a ₂	τ ₂ (ps)	a ₃	τ ₃ (ps)
0	0.480	0.200	0.120	0.680	0.400	4.90
50	0.490	0.220	0.0900	0.730	0.420	7.10
100	0.490	0.250	0.0600	0.790	0.450	8.20
150	0.470	0.270	0.0500	0.850	0.480	7.60
200	0.450	0.260	0.0600	0.630	0.490	5.90

[BSA] (g/L)	a₁	τ₁ (ps)	a₂	τ₂ (ps)	a₃	τ₃ (ps)
0	0.480	0.200	0.120	0.680	0.400	4.90
25	0.450	0.230	0.0900	0.700	0.460	30.0
50	0.460	0.260	0.100	0.750	0.440	99.0
75	0.450	0.290	0.0800	0.770	0.470	113
100	0.470	0.270	0.0700	0.810	0.460	127
125	0.460	0.250	0.0700	0.740	0.470	72.0
150	0.430	0.230	0.0900	0.640	0.480	25.0

[β-LG] (g/L)	a₁	τ₁ (ps)	a₂	τ₂ (ps)	a₃	τ₃ (ps)
0	0.480	0.200	0.120	0.680	0.400	4.90
25	0.440	0.220	0.100	0.660	0.460	16.0
50	0.440	0.240	0.0900	0.720	0.470	29.0
75	0.430	0.270	0.0800	0.750	0.490	35.0
100	0.460	0.230	0.0700	0.690	0.470	31.0
125	0.460	0.210	0.0800	0.650	0.460	27.0
150	0.470	0.180	0.0700	0.580	0.460	22.0

[Glucose] (g/L)	a₁	τ₁ (ps)	a₂	τ₂ (ps)	a₃	τ₃ (ps)
0	0.480	0.200	0.120	0.680	0.400	4.90
50	0.480	0.230	0.110	0.860	0.410	6.10
100	0.470	0.270	0.110	0.770	0.420	6.60
150	0.490	0.290	0.0800	0.840	0.430	7.30
200	0.500	0.320	0.0600	0.630	0.440	7.50

[Sucrose] (g/L)	a_1	τ_1 (ps)	a_2	τ_2 (ps)	a_3	τ_3 (ps)
0	0.480	0.200	0.120	0.680	0.400	4.90
50	0.480	0.260	0.100	0.760	0.420	7.30
100	0.490	0.290	0.0800	0.890	0.430	11.2
150	0.500	0.250	0.0700	0.740	0.430	9.40
200	0.500	0.210	0.0900	0.690	0.410	8.20

[Ethylene Glycol] (g/L)	a_1	τ_1 (ps)	a_2	τ_2 (ps)	a_3	τ_3 (ps)
0	0.480	0.200	0.120	0.680	0.400	4.90
50	0.490	0.260	0.080	0.710	0.430	6.20
100	0.490	0.290	0.090	0.860	0.420	6.90
150	0.500	0.320	0.080	0.910	0.420	7.50
200	0.500	0.370	0.060	1.30	0.440	7.60

Table S10: The principal components obtained from singular value decomposition (SVD) of the transient absorption data for ferric Cyt *c* in buffer and in the presence of synthetic monomeric crowders (Independent experiments with ~ 10 % error).

Crowder (g/L)	Glucose				Sucrose				Ethylene Glycol			
	τ_1 (ps)	τ_2 (ps)	τ_3 (ps)	τ_4 (ps)	τ_1 (ps)	τ_2 (ps)	τ_3 (ps)	τ_4 (ps)	τ_1 (ps)	τ_2 (ps)	τ_3 (ps)	τ_4 (ps)
0	0.120 ±0.010	0.330 ±0.110	5.00 ±1.10	9.18 ±1.01	0.120 ±0.010	0.330 ±0.110	5.00 ±1.25	9.18 ±1.01	0.120 ±0.010	0.330 ±0.110	5.00 ±1.30	9.18 ±1.01
50	0.120 ±0.020	0.390 ±0.160	4.18 ±1.11	10.4 ±1.4	0.120 ±0.010	0.520 ±0.050	3.91 ±0.40	11.7 ±1.2	0.140 ±0.010	0.370 ±0.040	4.09 ±0.39	12.1 ±1.5
100	0.120 ±0.020	0.440 ±0.190	4.04 ±1.07	15.4 ±2.0	0.190 ±0.020	0.630 ±0.060	4.15 ±0.41	23.5 ±2.5	0.160 ±0.020	0.260 ±0.030	4.30 ±0.41	19.1 ±1.9
150	0.220 ±0.020	0.540 ±0.210	4.47 ±0.62	92.5 ±5.0	0.160 ±0.020	0.230 ±0.020	3.95 ±0.37	19.1 ±2.1	0.190 ±0.020	0.420 ±0.050	4.30 ±0.36	23.1 ±1.9
200	0.110 ±0.010	0.650 ±0.230	5.03 ±1.23	163.9 ±8.5	0.150 ±0.010	0.260 ±0.020	3.84 ±0.42	15.7 ±1.7	0.200 ±0.020	0.650 ±0.060	4.96 ±0.60	28.1 ±2.5

Table S11: The principal components obtained from singular value decomposition (SVD) of the transient absorption data for ferrous Cyt *c* in buffer and in the presence of synthetic monomeric crowders (Independent experiments with ~ 10 % error).

Crowder (g/L)	Glucose				Sucrose				Ethylene Glycol			
	τ_1 (ps)	τ_2 (ps)	τ_3 (ps)	τ_4 (ps)	τ_1 (ps)	τ_2 (ps)	τ_3 (ps)	τ_4 (ps)	τ_1 (ps)	τ_2 (ps)	τ_3 (ps)	τ_4 (ps)
0	0.220 ±0.410	0.560 ±0.070	2.77 ±0.16	7.20 ±1.06	0.220 ±0.410	0.560 ±0.070	2.77 ±0.16	7.20 ±1.06	0.220 ±0.410	0.560 ±0.070	2.77 ±0.16	7.20 ±1.06
50	0.240 ±0.030	1.57 ±0.18	4.72 ±0.49	10.7 ±1.3	0.290 ±0.030	0.650 ±0.070	3.88 ±0.41	12.1 ±1.3	0.260 ±0.020	0.600 ±0.050	4.82 ±0.52	8.98 ±0.93
100	0.260 ±0.030	0.690 ±0.070	4.82 ±0.46	13.3 ±1.4	0.340 ±0.040	0.800 ±0.070	5.48 ±0.61	21.9 ±2.0	0.300 ±0.030	0.810 ±0.080	5.52 ±0.58	10.1 ±1.1
150	0.280 ±0.030	1.00 ±0.09	5.55 ±0.62	15.4 ±1.6	0.320 ±0.030	0.580 ±0.050	4.40 ±0.46	17.8 ±1.6	0.340 ±0.030	0.890 ±0.090	6.03 ±0.65	12.1 ±1.3
200	0.310 ±0.030	0.670 ±0.060	5.20 ±0.53	20.4 ±1.9	0.320 ±0.030	0.440 ±0.040	4.63 ±0.49	15.9 ±1.5	0.400 ±0.040	1.01 ±0.01	4.25 ±0.42	15.2 ±1.7

Table S12: The principal components obtained from singular value decomposition (SVD) of the transient absorption data for ferric Cyt *c* in buffer and in the presence of protein crowders (Independent experiments with ~ 10 % error).

Crowder (g/L)	Bovine Serum Albumin				β -Lactoglobulin			
	τ_1 (ps)	τ_2 (ps)	τ_3 (ps)	τ_4 (ps)	τ_1 (ps)	τ_2 (ps)	τ_3 (ps)	τ_4 (ps)
0	0.120±0.010	0.330±0.110	5.00±1.30	9.18±1.01	0.120±0.010	0.330±0.110	5.00±1.25	9.18±1.01
25	0.150±0.010	0.420±0.050	5.58±0.62	236.1±25.6	0.120±0.010	0.390±0.040	3.90±0.38	123.0±11.6
50	0.170±0.020	0.480±0.050	6.83±0.65	318.5±33.1	0.140±0.010	0.420±0.050	4.35±0.42	159.6±14.5
75	0.190±0.020	0.540±0.060	7.48±0.75	732.2±75.2	0.150±0.010	0.440±0.050	3.86±0.36	224.4±21.3
100	0.260±0.030	0.640±0.060	6.51±0.59	1178±101	0.210±0.020	0.480±0.050	3.81±0.37	442.2±39.5
125	0.220±0.020	0.460±0.050	3.89±0.41	145.2±11.2	0.190±0.020	0.460±0.040	4.09±0.39	106.6±9.8
150	0.200±0.020	0.400±0.040	3.53±0.38	56.0±4.5	0.130±0.010	0.280±0.030	4.17±0.39	84.0±7.6

Table S13: The principal components obtained from singular value decomposition (SVD) of the transient absorption data for ferrous Cyt *c* in buffer and in the presence of protein crowders (Independent experiments with ~ 10 % error).

Crowder (g/L)	Bovine Serum Albumin				β -Lactoglobulin			
	τ_1 (ps)	τ_2 (ps)	τ_3 (ps)	τ_4 (ps)	τ_1 (ps)	τ_2 (ps)	τ_3 (ps)	τ_4 (ps)
0	0.220±0.410	0.560±0.070	2.77±0.16	7.20±1.06	0.220±0.410	0.560±0.070	2.77±0.16	7.20±1.06
25	0.260±0.030	0.600±0.060	5.93±0.57	117.1±12.3	0.250±0.020	0.580±0.060	4.98±0.51	39.6±3.5
50	0.300±0.030	0.670±0.060	5.96±0.61	465.0±44.1	0.290±0.030	0.620±0.060	5.48±0.57	83.9±8.7
75	0.340±0.040	0.720±0.070	5.85±0.56	511.0±47.6	0.320±0.030	0.640±0.060	5.45±0.55	113.8±10.3
100	0.360±0.040	0.790±0.080	6.32±0.61	746.3±73.2	0.300±0.030	0.600±0.060	5.41±0.51	97.7±8.3
125	0.290±0.030	0.550±0.060	5.49±0.53	333.1±32.6	0.290±0.030	0.590±0.050	5.19±0.49	73.7±6.7
150	0.230±0.020	0.520±0.050	5.09±0.49	78.9±7.6	0.240±0.020	0.570±0.050	5.18±0.56	58.2±8.3

Table S14: Amplitudes obtained from decay kinetics of ferric Cyt *c*, probed at 600 nm in the buffer as a function of increasing pump power.

Components \ Pump Power	0.120 (ps)	0.360 (ps)	3.65 (ps)	6.22 (ps)	Inf >8 ns
0.3 mW	0.530	0.0600	0.260	0.150	0.0000600
0.5 mW	0.514	0.0700	0.255	0.170	0.000100
0.6 mW	0.558	0.0950	0.228	0.110	0.00900
0.7 mW	0.560	0.0800	0.270	0.0800	0.0100
0.9 mW	0.560	0.0900	0.280	0.0500	0.0200
1.1 mW	0.570	0.0700	0.290	0.0500	0.0200

Table S15: Amplitudes obtained from decay kinetics of ferrous Cyt *c*, probing at 575 nm in the buffer as a function of increasing pump power.

Components Pump Power \	0.270 (ps)	0.610 (ps)	2.30 (ps)	6.80 (ps)	Inf >8 ns
0.1 mW	0.470	0.100	0.230	0.200	0.0000100
0.2 mW	0.480	0.110	0.240	0.170	0.0000240
0.3 mW	0.500	0.120	0.250	0.130	0.0000370
0.5 mW	0.510	0.120	0.270	0.100	0.0000800
0.7 mW	0.525	0.130	0.270	0.0480	0.0270
0.8 mW	0.531	0.130	0.275	0.0330	0.0310

Figure S1.1 – Ground state absorption spectra of ferric Cytochrome *c* in presence of (A) Dextran 40, (B) Ficoll 70, (C) PEG 8 and (D) Dextran 70 (Dashed arrow in blue indicating the pump wavelength 400 nm).

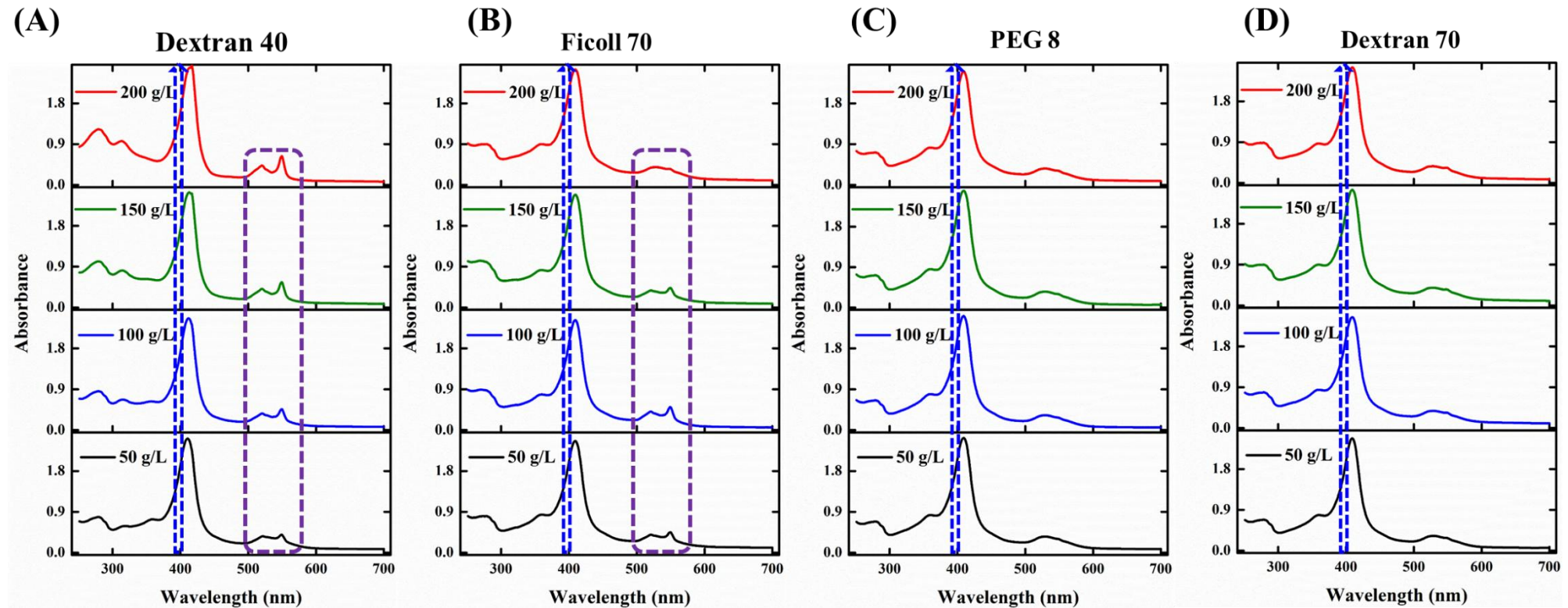


Figure S1.2 – Ground state absorption spectra of ferrous Cytochrome *c* in presence of (A) Dextran 40, (B) Ficoll 70, (C) PEG 8 and (D) Dextran 70 (Dashed arrow in blue indicating the pump wavelength 400 nm).

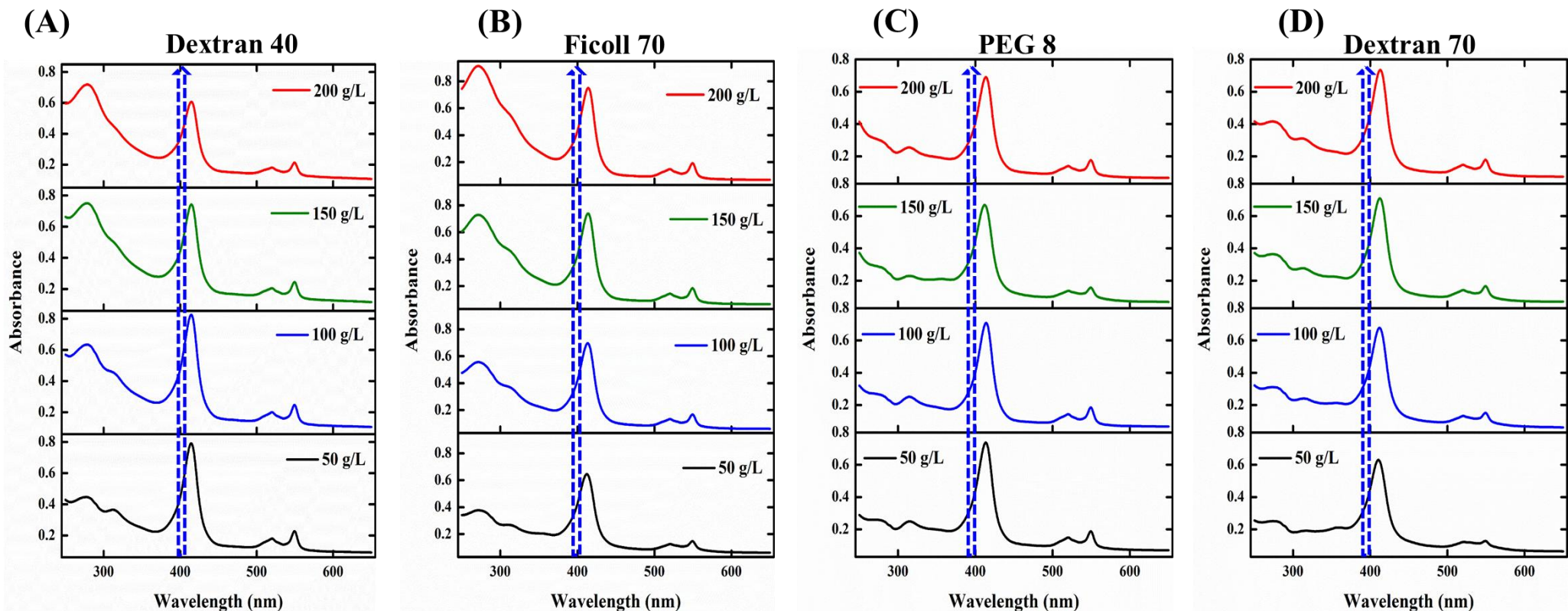


Figure S1.3 – Ground state absorption spectra of ferric Cytochrome *c* in presence of (A) Glucose, (B) Sucrose, and (C) Ethylene Glycol (Dashed arrow in blue indicating the pump wavelength 400 nm).

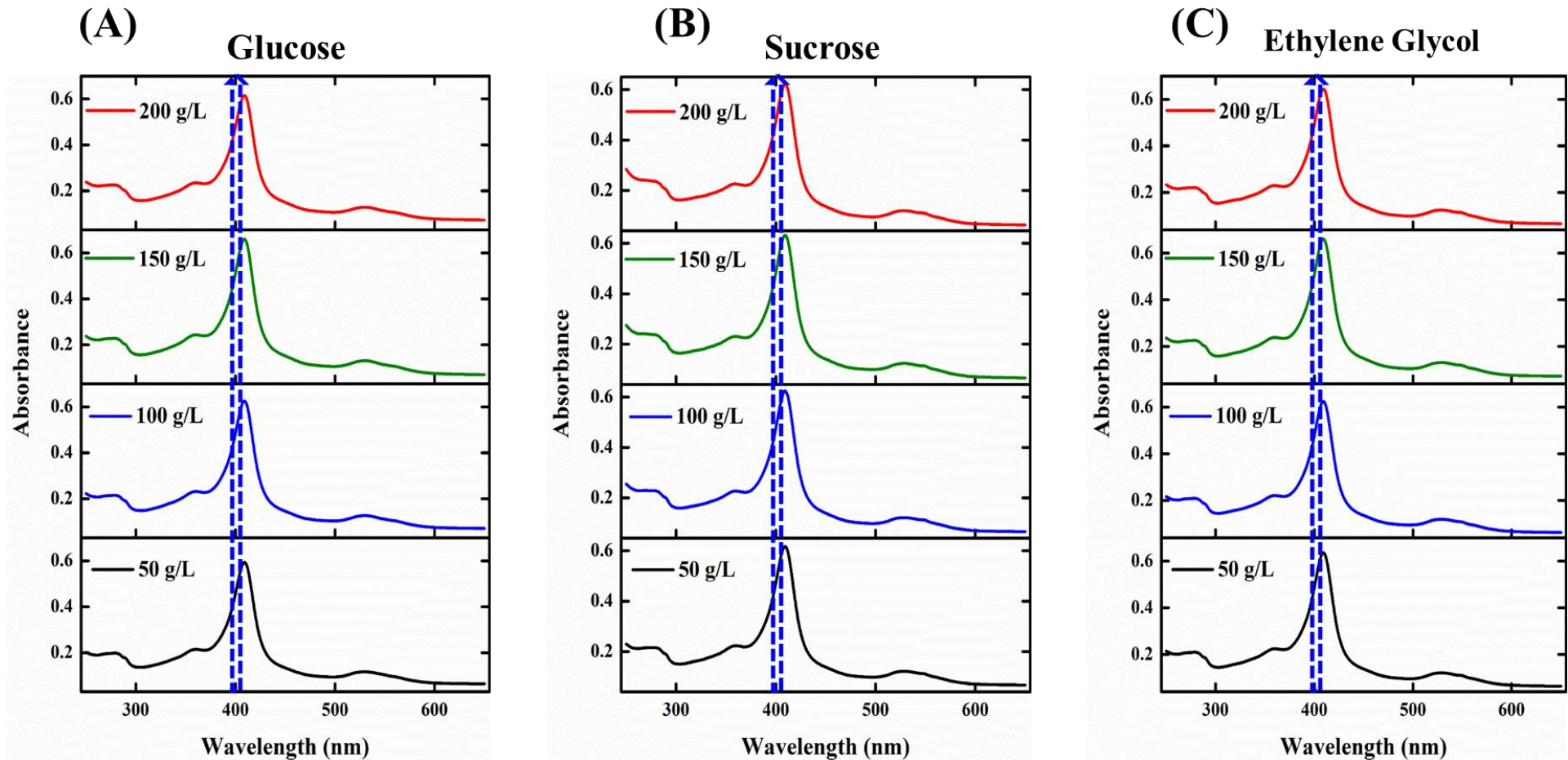


Figure S1.4 – Ground state absorption spectra of ferrous Cytochrome *c* in presence of (A) Glucose, (B) Sucrose, and (C) Ethylene Glycol (Dashed arrow in blue indicating the pump wavelength 400 nm).

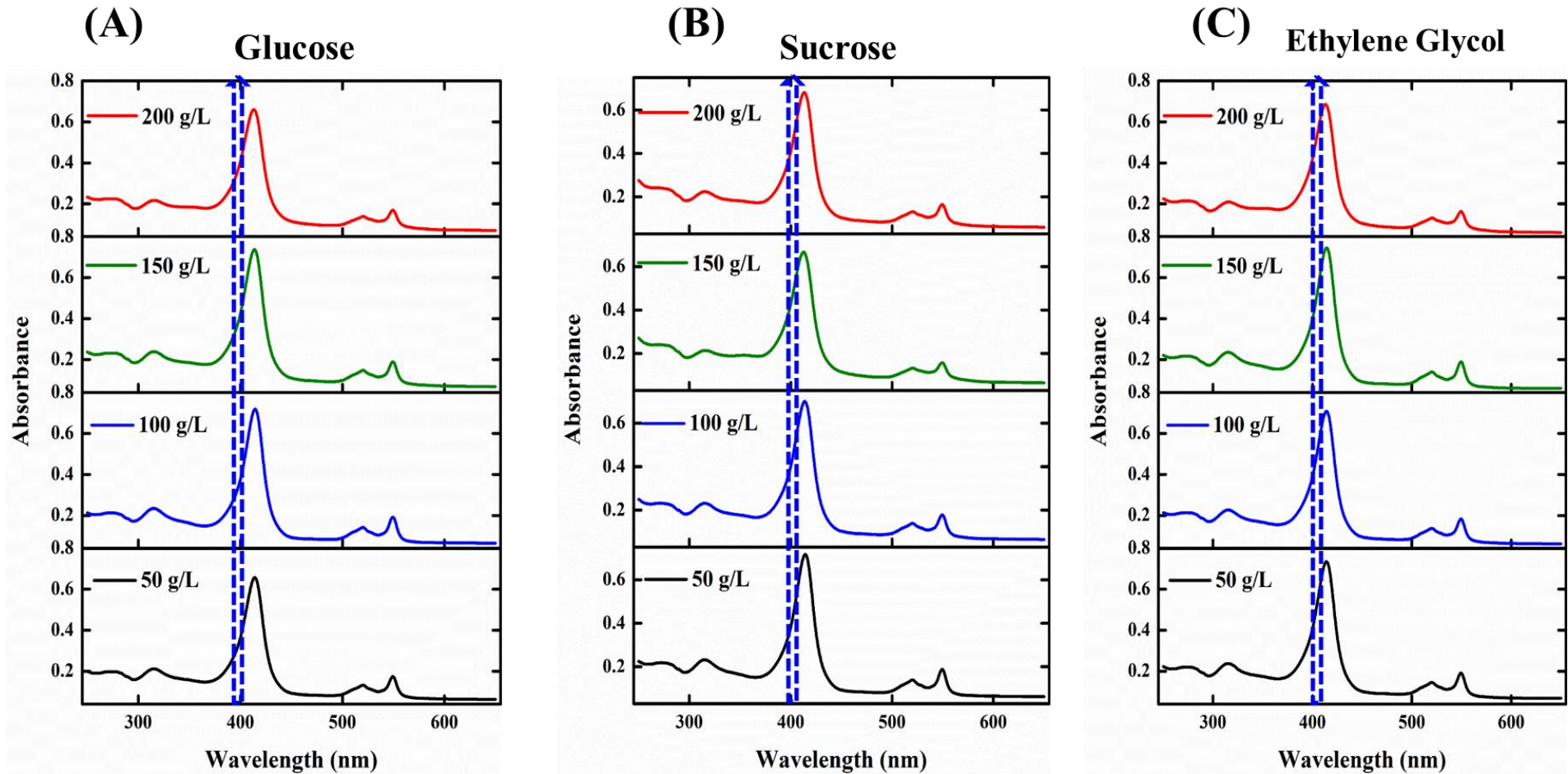


Figure S1.5 – Ground state absorption spectra of (A) ferric and (B) ferrous Cytochrome *c* in presence of BSA as crowder and (C) ferric and (D) ferrous Cyt *c* in presence of β -LG as crowder (Dashed arrow in blue indicating the pump wavelength 400 nm).

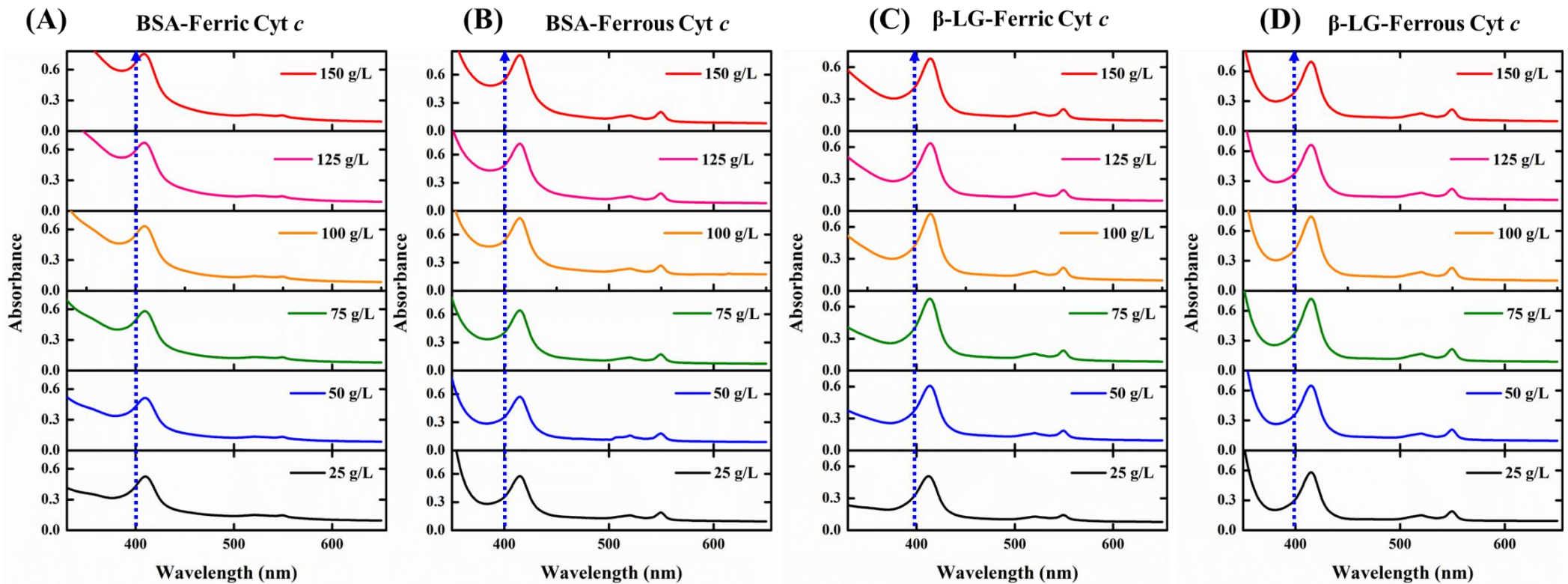


Figure S2 – Transient Absorption Spectra of Fe³⁺ cyt c in presence of Crowders, [A-D] Dextran 40, [E-H] Ficoll 70, [I-L] PEG 8 and [M-P] Dextran 70 at varying concentration from 50 to 200 g/L.

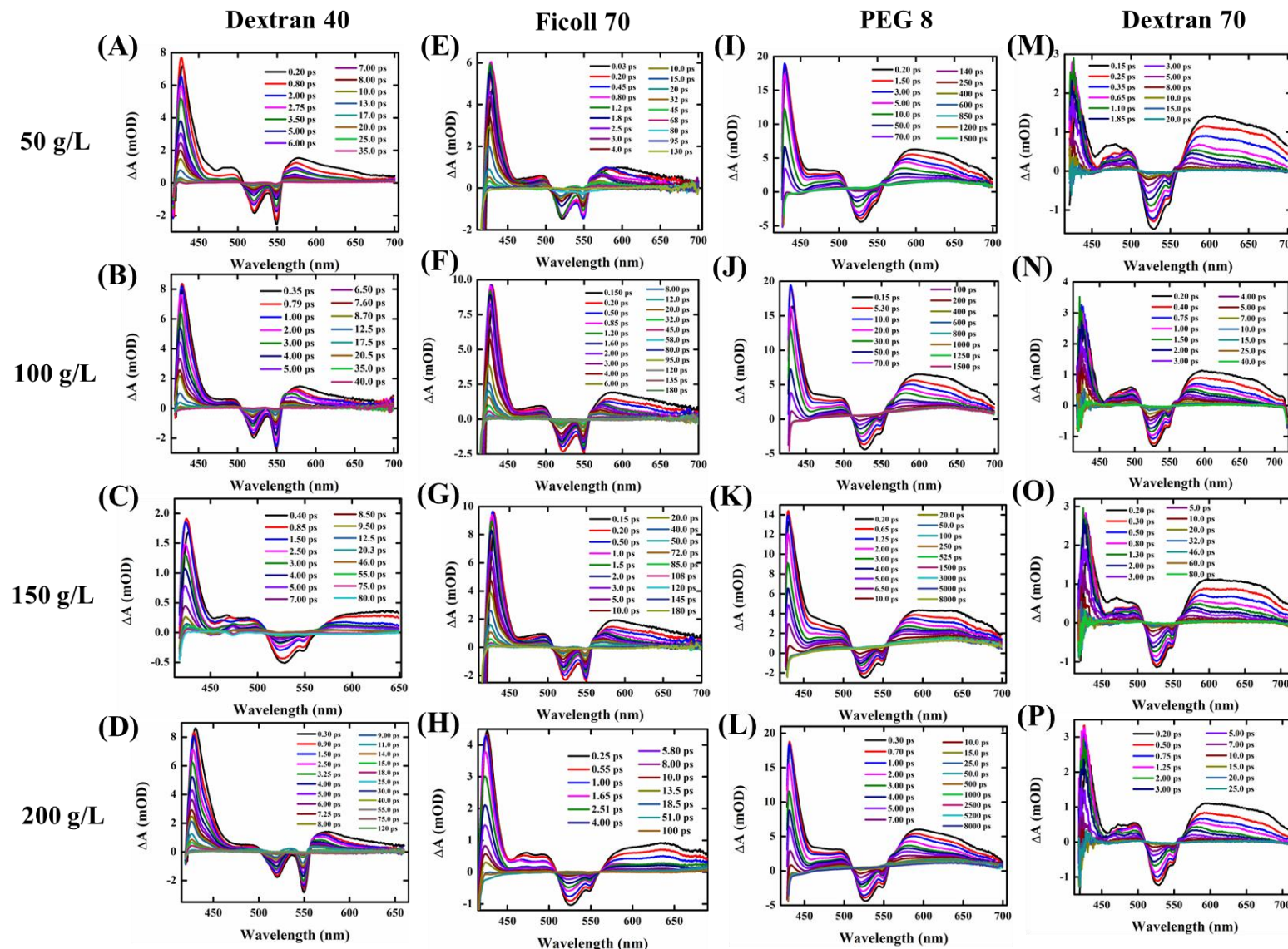


Figure S3 – Single Wavelength Kinetics Spectra of Fe^{3+} cytochrome *c* probed at 600 nm in the presence of synthetic crowders, (A) Dextran 40, (B) Dextran 70, (C) Ficoll 70, (D) PEG 8, (E) Glucose, (F) Sucrose and (G) Ethylene glycol.

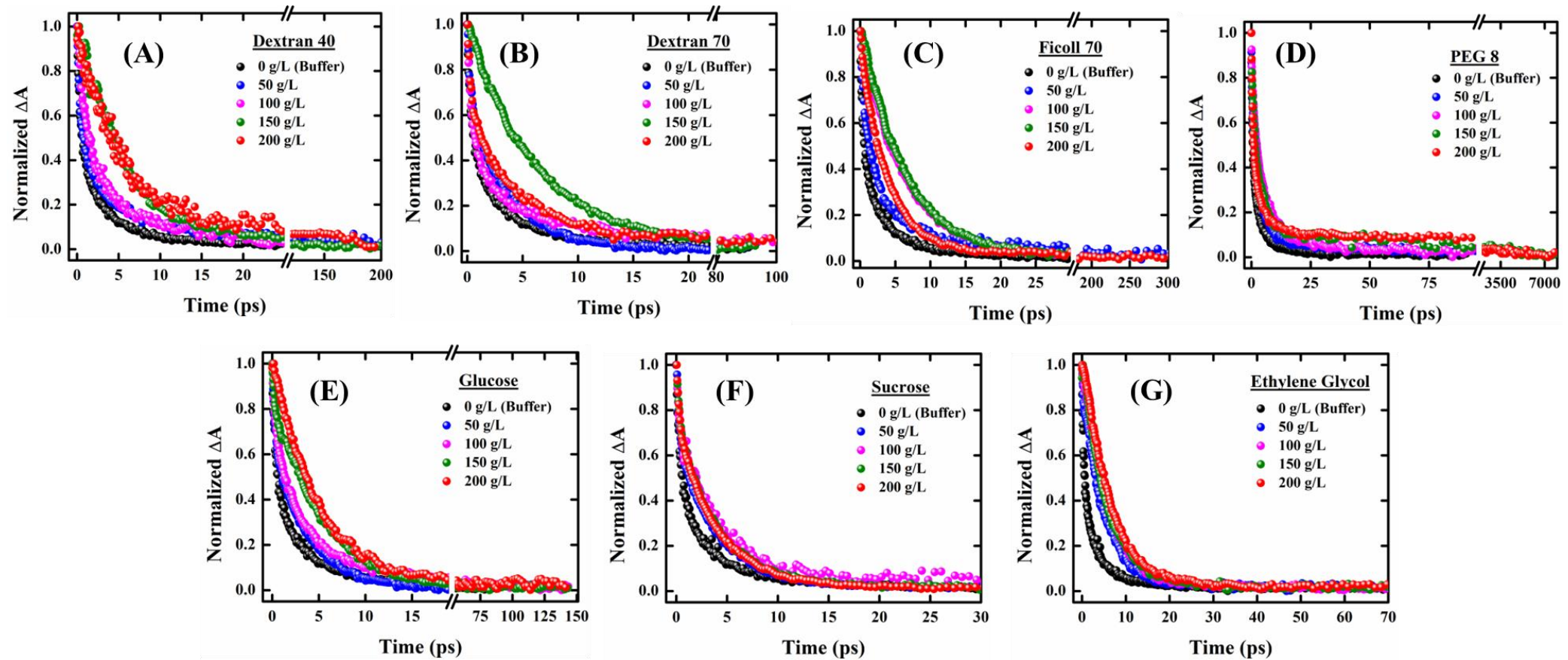


Figure S4 – Comparison of (i) ground state absorption spectra and DAS of excited state decay (τ_1) of heme of (A) ferric, (B) ferrous in the buffer. (ii) transient absorption spectra at early time delay (0.15 ps) and DAS of τ_2 component for (C) ferric and (D) DAS of both τ_2 and τ_3 components for Ferrous. (iii) Methionine rebinding DAS (τ_4) of ferrous with (E) Differential ground state absorption of ferric and ferrous and (F) Ground state absorption spectra of ferrous Cyt c in the buffer.

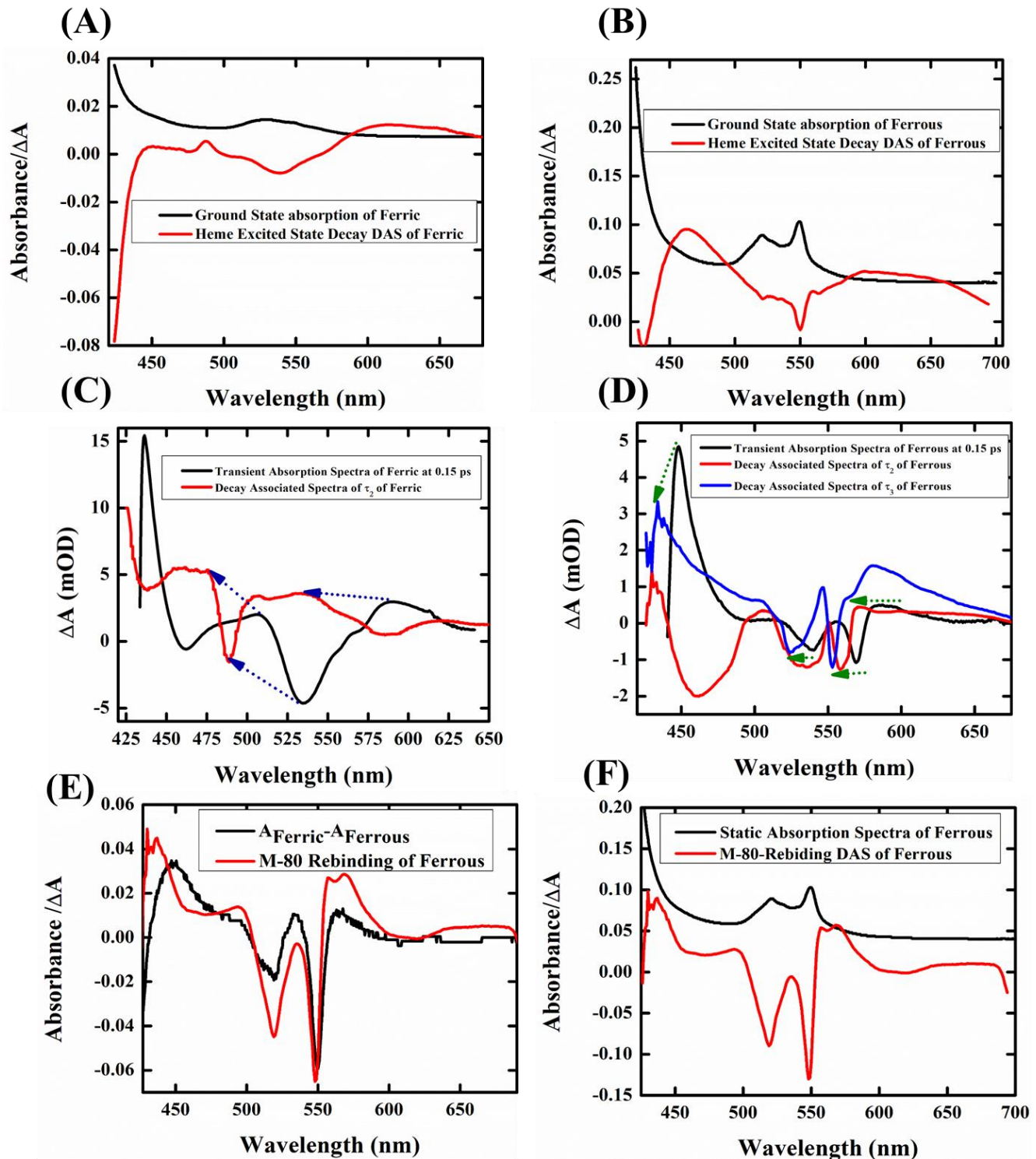


Figure S5: Transient absorption spectra of (A) ferric and (B) ferrous Cyt *c* in buffer exhibiting vibrational cooling through spectral blue shift and narrowing of bands.

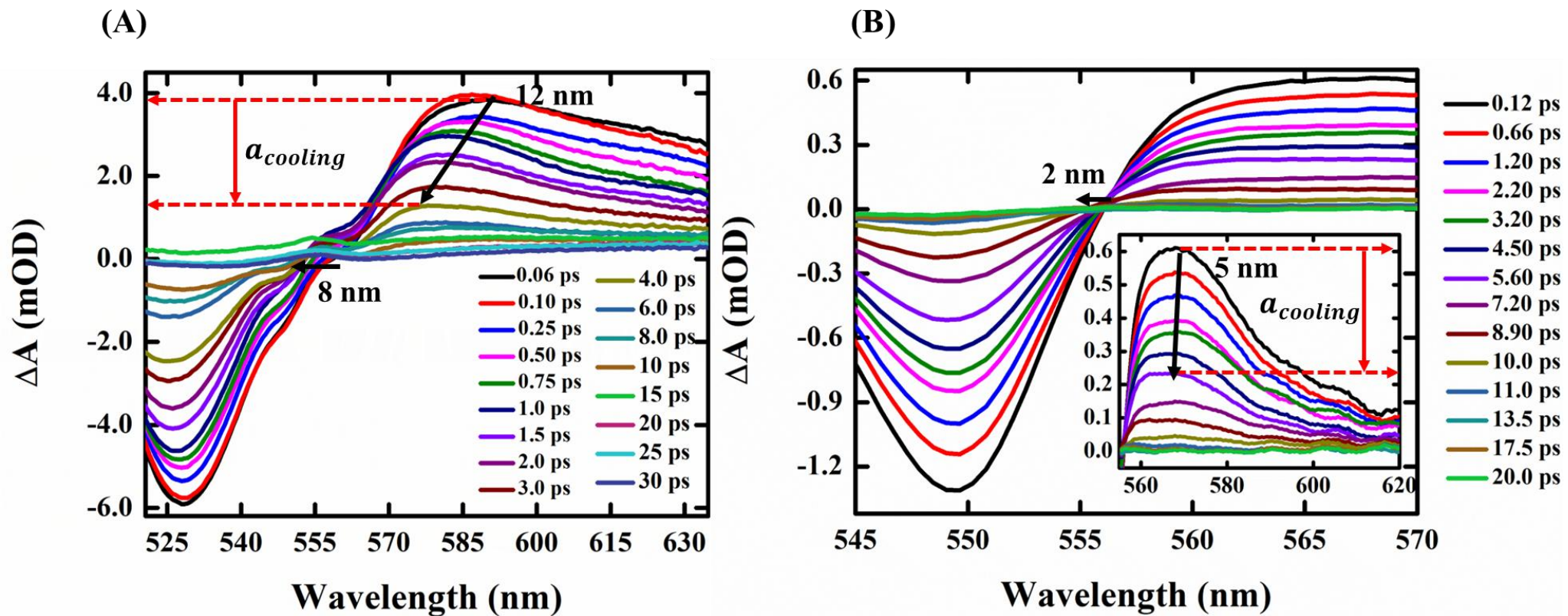


Figure S6: Overlapped transient absorption decay of (A-J) ferric (435 and 600 nm) and (K-T) ferrous Cyt c (430 and 575 nm) in buffer and in the presence of PEG 8 [(B-F) and (L-O)] and BSA [(F-J) and (P-T)].

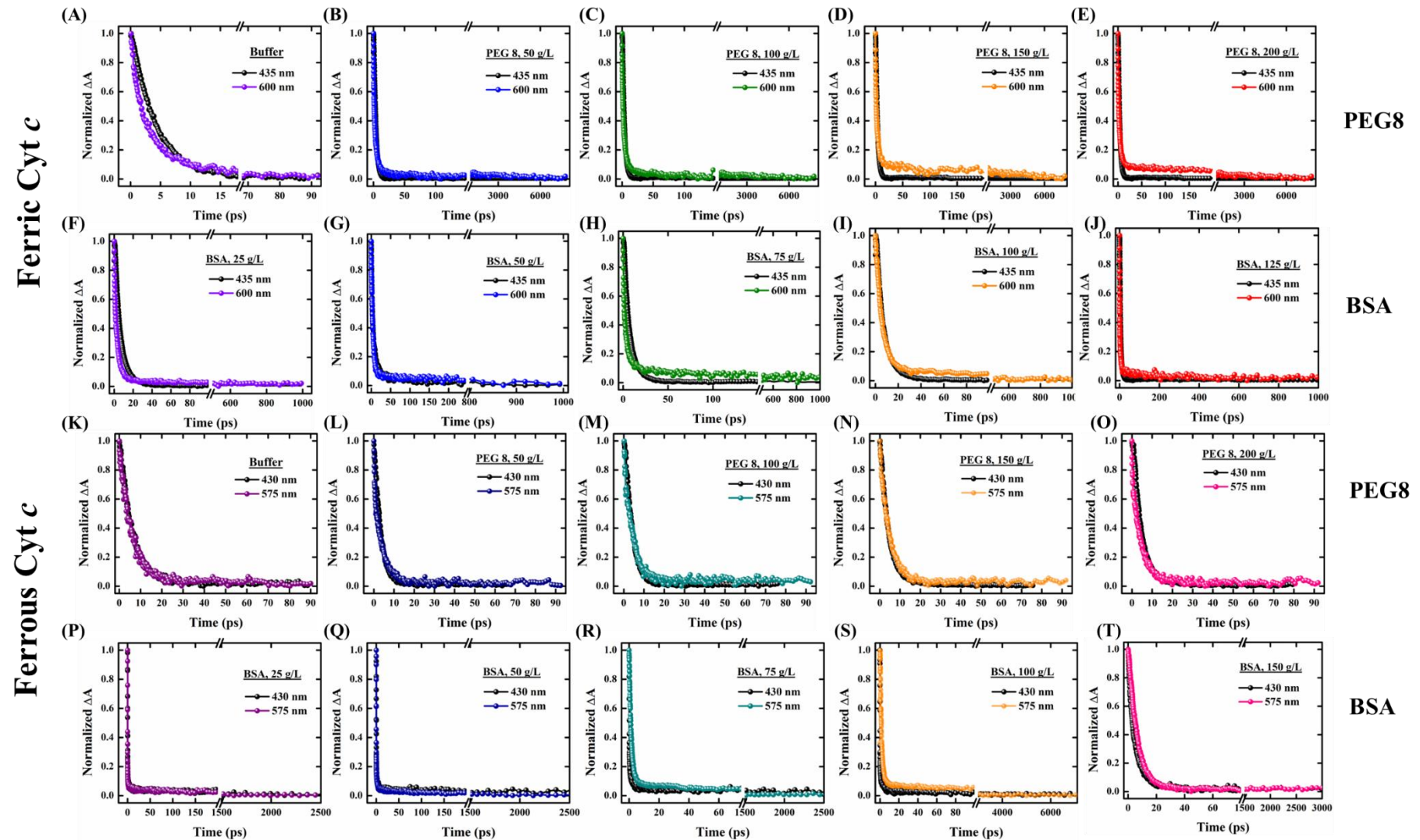


Figure S7 – Normalized Decay Associated Spectra of ferric Cytochrome *c* in presence of buffer, (A - D) PEG 8, (E - H) Ficoll 70, (I – L) Dextran 40 and (M - P) Dextran 70.

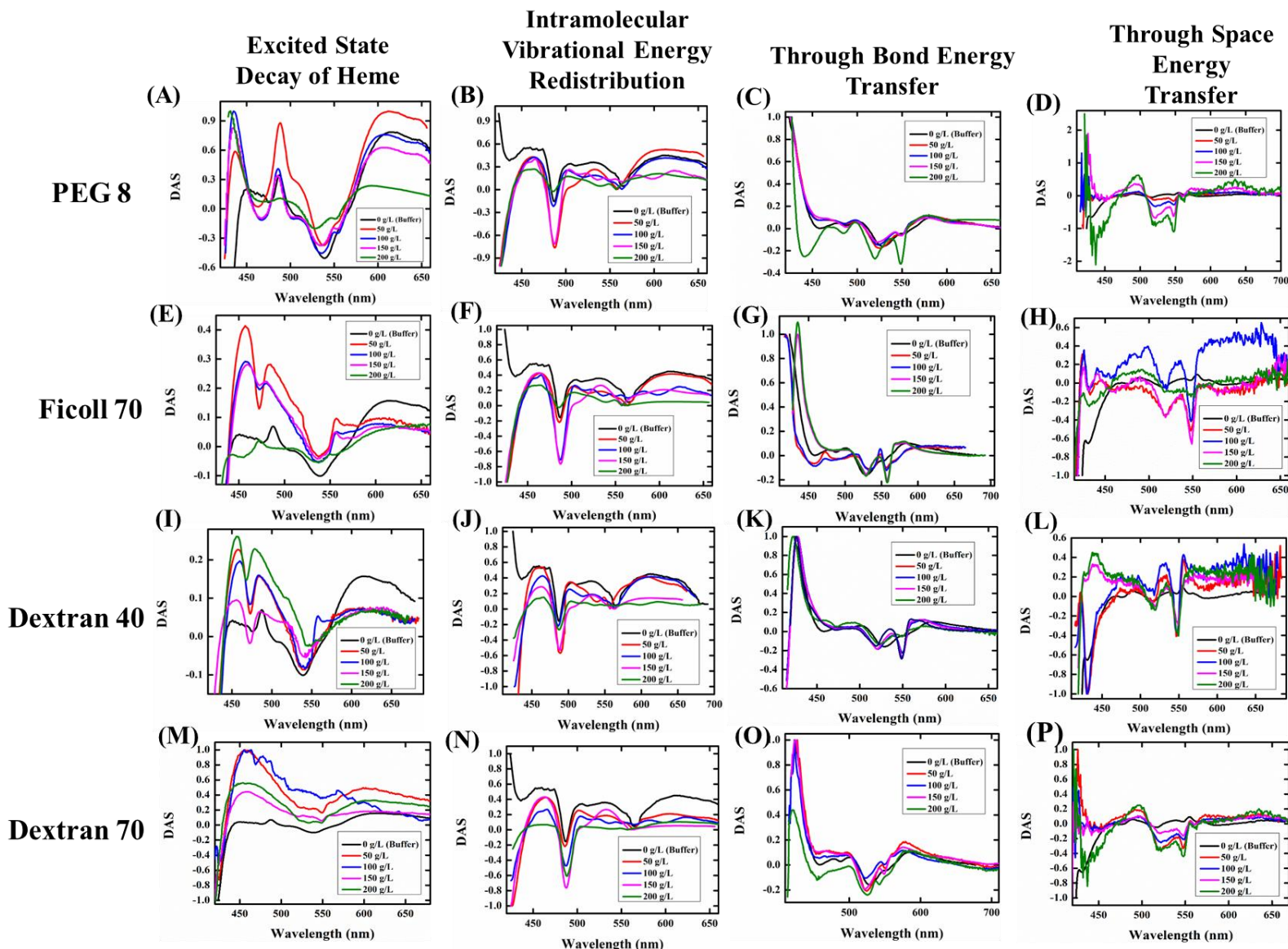


Figure S8 – Normalized Decay Associated Spectra of ferrous Cytochrome *c* in presence of buffer, (A - D) PEG 8, (E - H) Ficoll 70, (I – L) Dextran 40 and (M - P) Dextran 70.

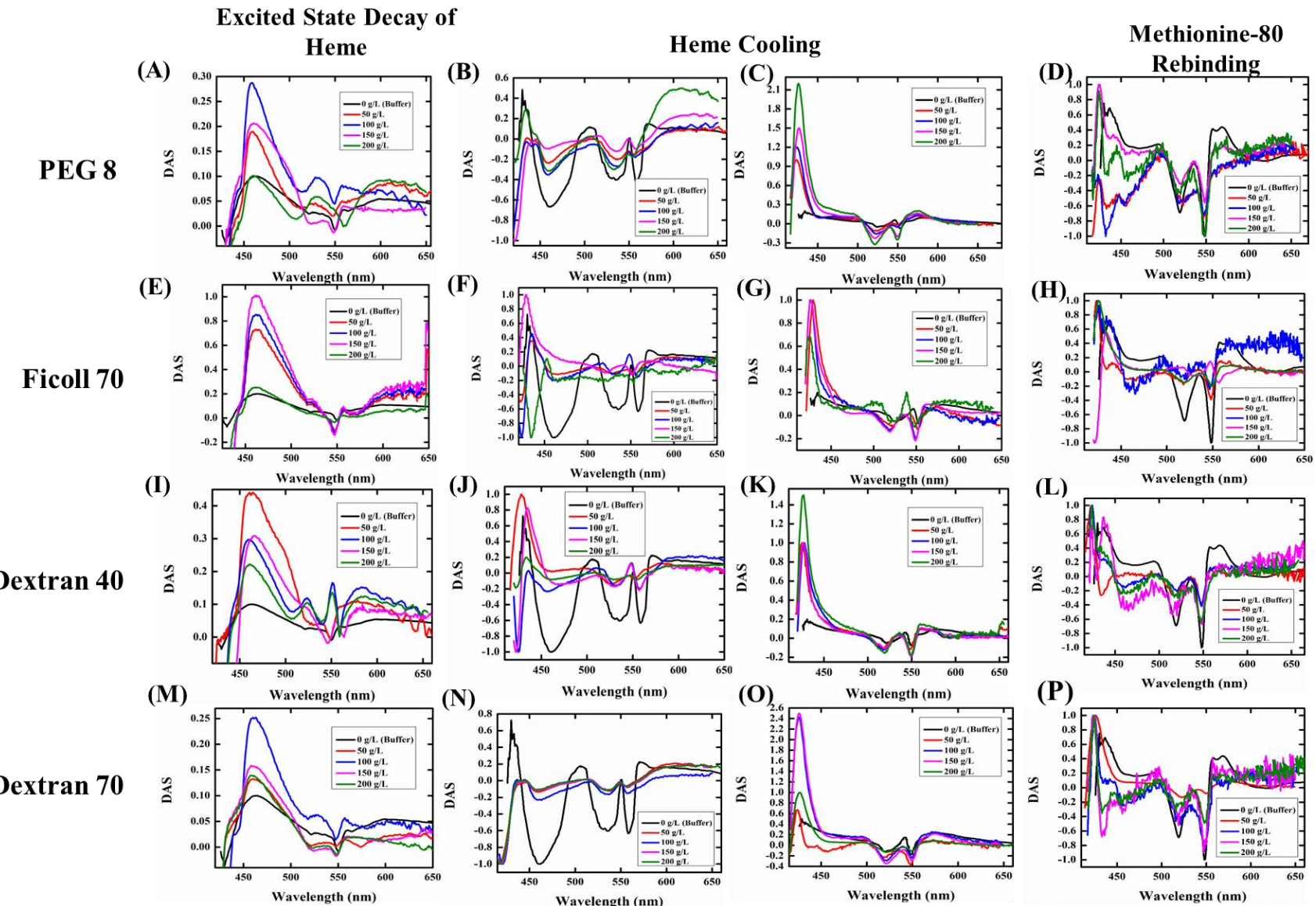


Figure S9 – Comparison of transient absorption spectra at early time delay (0.15 ps) and (i) DAS of τ_2 component for ferric (A-H), (ii) DAS of both τ_2 and τ_3 components for ferrous (I-L) Cytochrome *c* in the presence of crowders as mentioned at the top (concentrations as mentioned to the left of the figure panels).

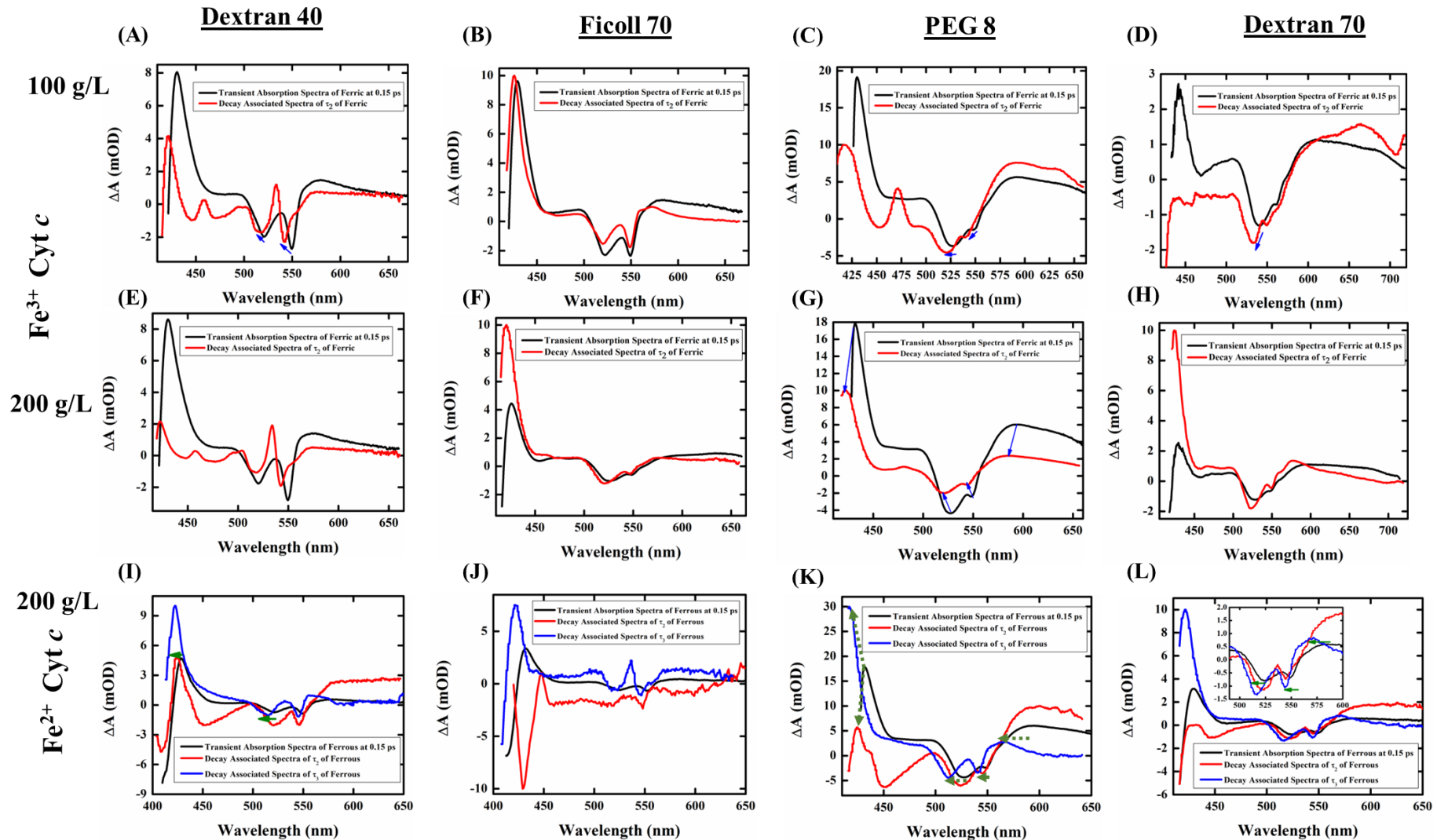


Figure S10 – Secondary structure of Fe^{3+} Cyt *c* obtained at 25 °C in the presence of buffer and synthetic polymeric crowders of (A) 100 g/L, (B) 200 g/L and Fe^{2+} Cyt *c* in the presence of crowders of (C) 100 g/L, (D) 200 g/L. Active site structure of Fe^{3+} Cyt *c* in the presence of buffer and crowders of (E) 100 g/L, (F) 200 g/L and Fe^{2+} Cyt *c* in the presence of crowders of (G) 100 g/L, (H) 200 g/L as mentioned in the panels, with the data points in the CD spectra shown being an average of four independent scans (error bars not shown for clarity of data).

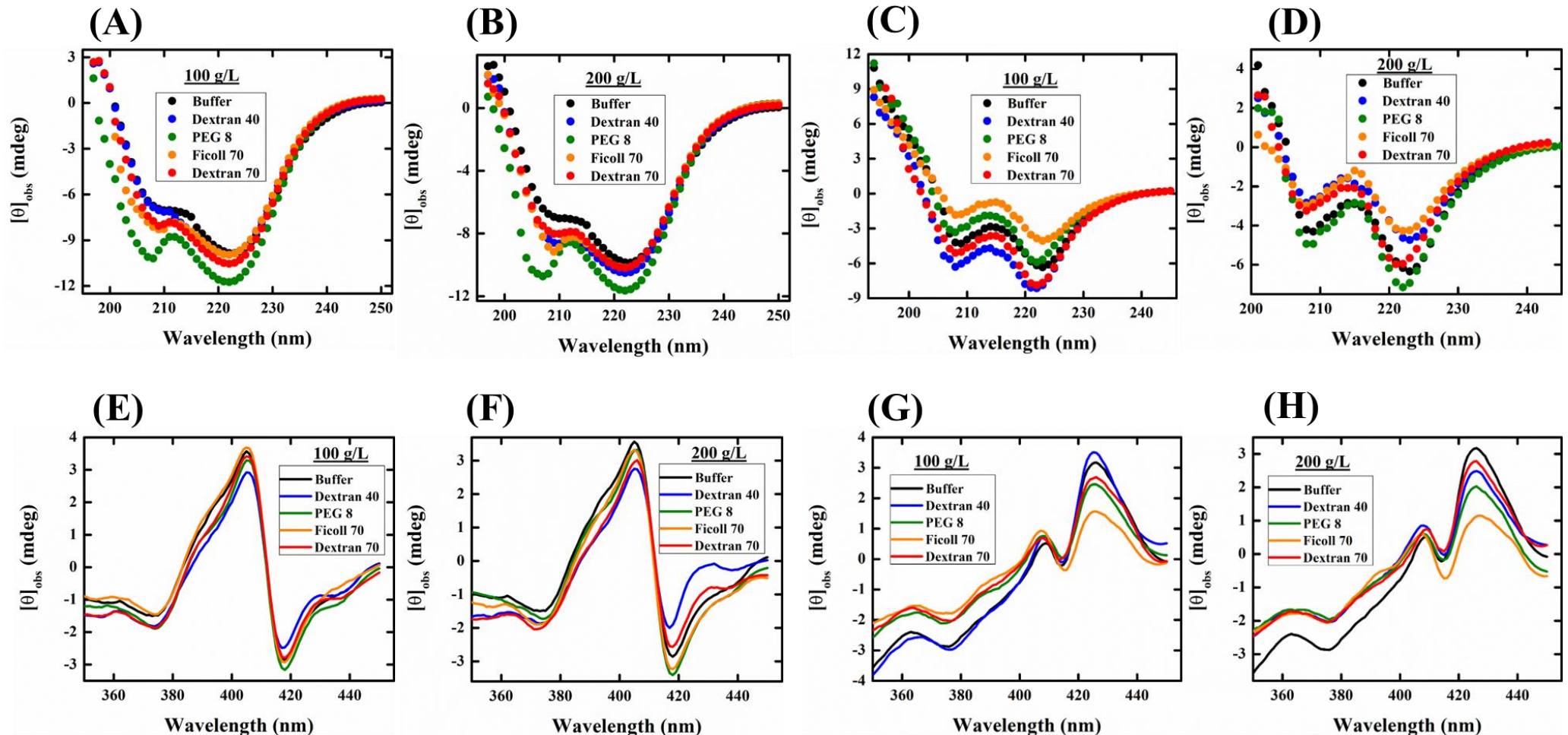


Figure S11 – Steady-state fluorescence spectra of ferric Cytochrome *c* (top panel) and ferrous Cytochrome *c* (bottom panel) in presence of buffer and crowders.

Fe³⁺ Cytochrome *c*

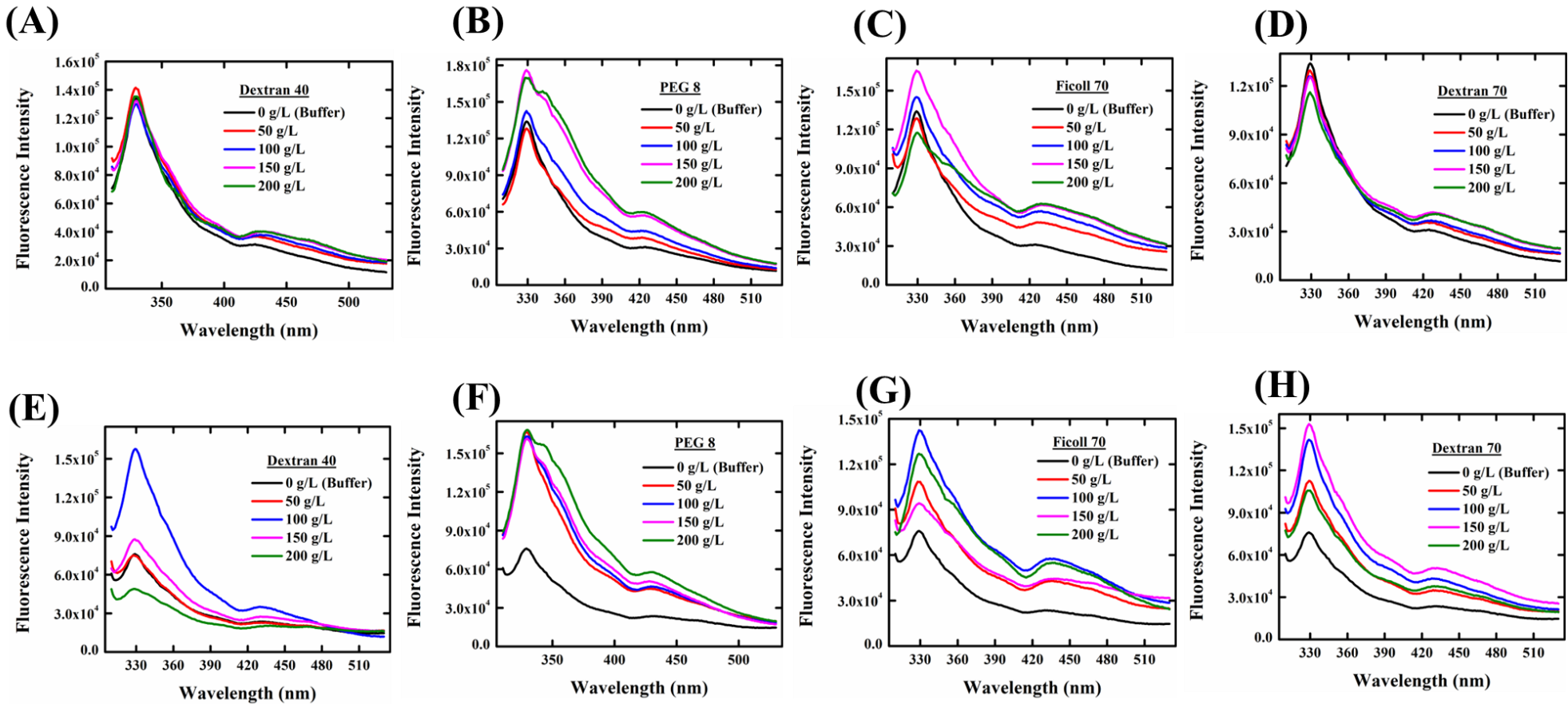


Figure S12 – Variation in τ_4 of ferric Cyt c as a function of crowder concentrations comparing the effects of (A) Glucose, Dextran 40 and Dextran 70, (B) Sucrose and Ficoll 70, (C) Ethylene glycol and PEG 8 and the similar comparison of ferrous Cyt c comparing (D) Glucose, Dextran 40 and Dextran 70, (E) Sucrose and Ficoll 70, (F) Ethylene glycol and PEG 8.

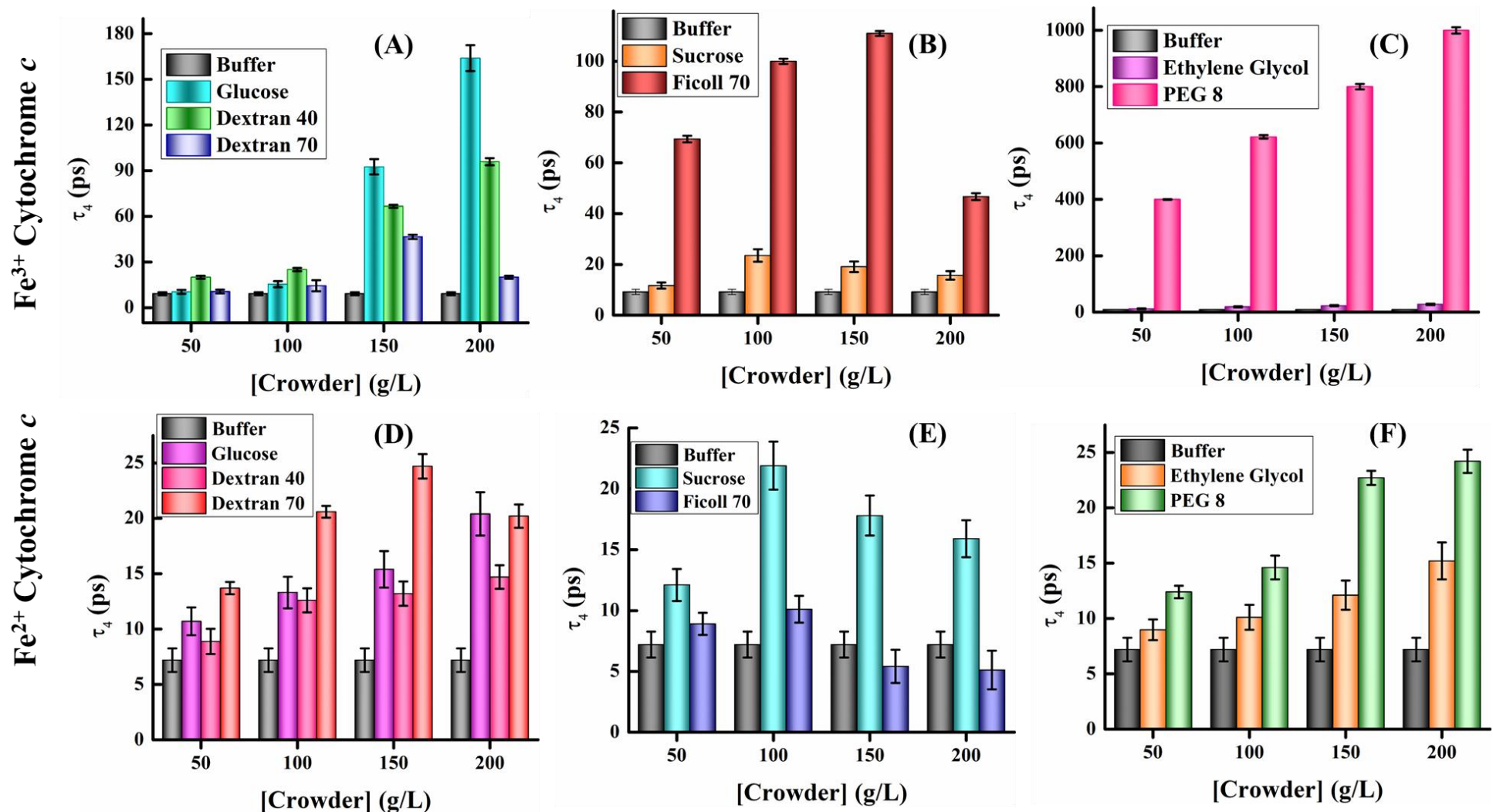


Figure S13 – Secondary structure of Fe^{3+} Cyt *c* obtained at 25 °C in the presence of buffer and small molecule crowders of (A) 100 g/L, (B) 200 g/L and Fe^{2+} Cyt *c* in the presence of crowders of (C) 100 g/L, (D) 200 g/L. Active site structure of Fe^{3+} Cyt *c* in the presence of buffer and crowders of (E) 100 g/L, (F) 200 g/L and Fe^{2+} Cyt *c* in the presence of crowders of (G) 100 g/L, (H) 200 g/L as mentioned in the panels, with the data points in the CD spectra shown being an average of four independent scans (error bars not shown for clarity of data).

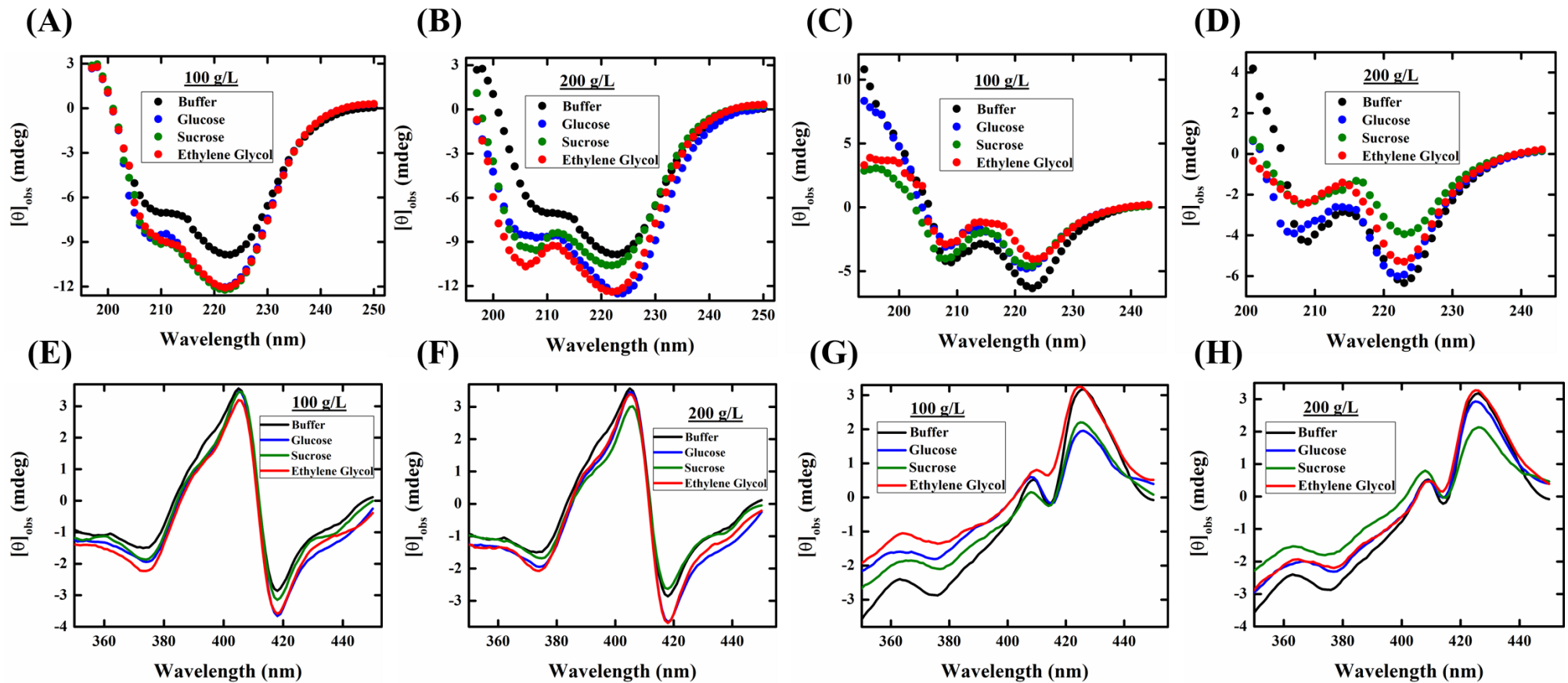


Figure S14 – Active site structure of Cyt *c* in the presence of buffer and protein-based crowders (BSA and β -LG) of (A) ferric and (B) ferrous form at 50 and 100 g/L as mentioned in the panels, with the data points in the CD spectra shown being an average of four independent scans (error bars not shown for clarity of data).

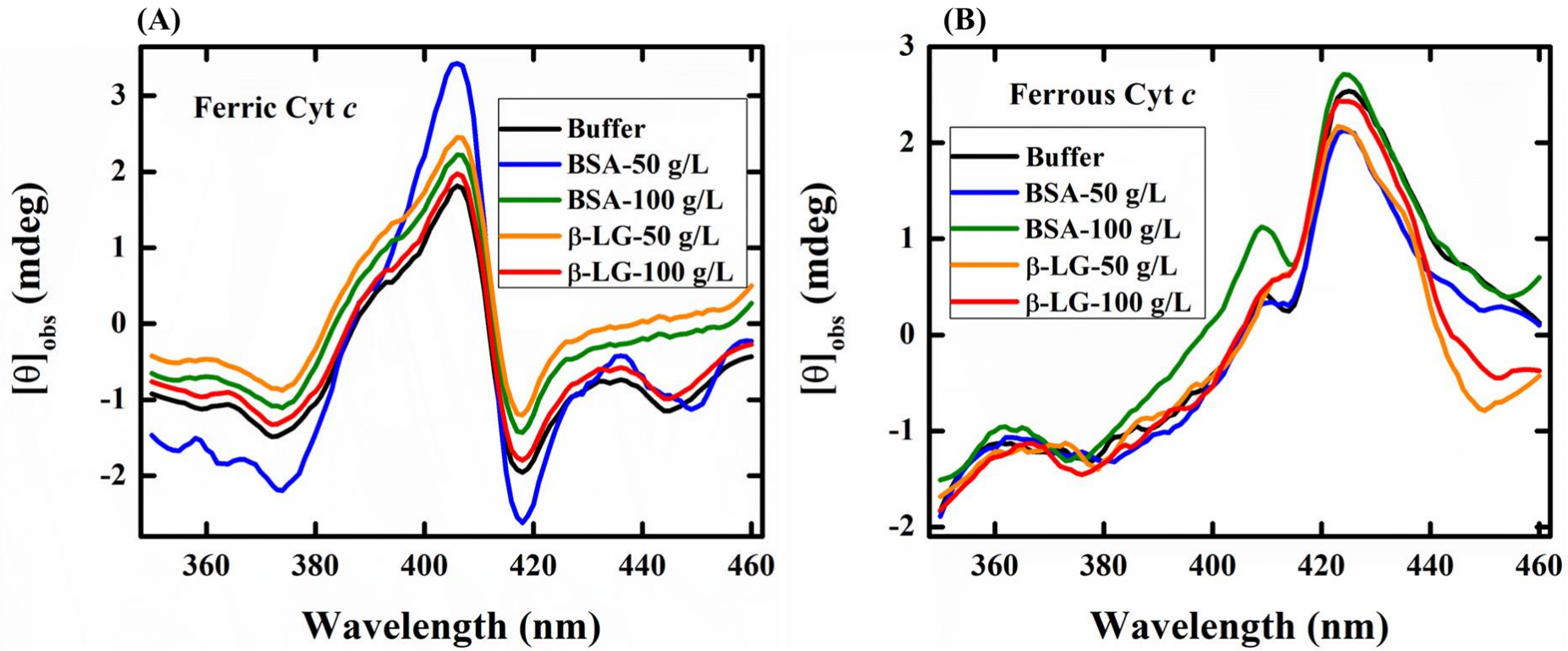


Figure 15 – Ground state absorption spectra of ferric Cytochrome *c* in the presence of (A) BSA and (B) β -LG as crowder (Dashed arrow in black indicating the shift in soret band as a function of crowder concentration) [Inset: Variation in absorbance of Q-band].

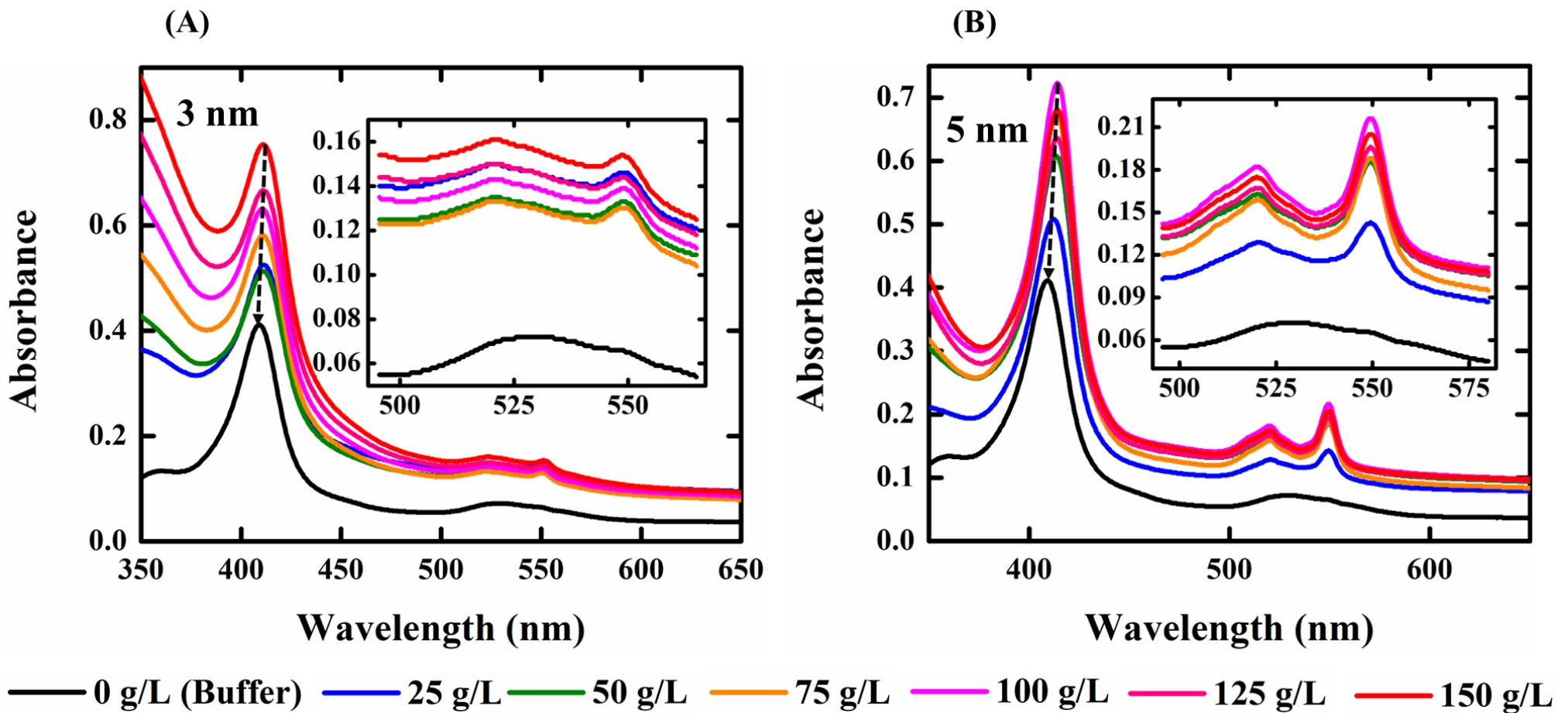
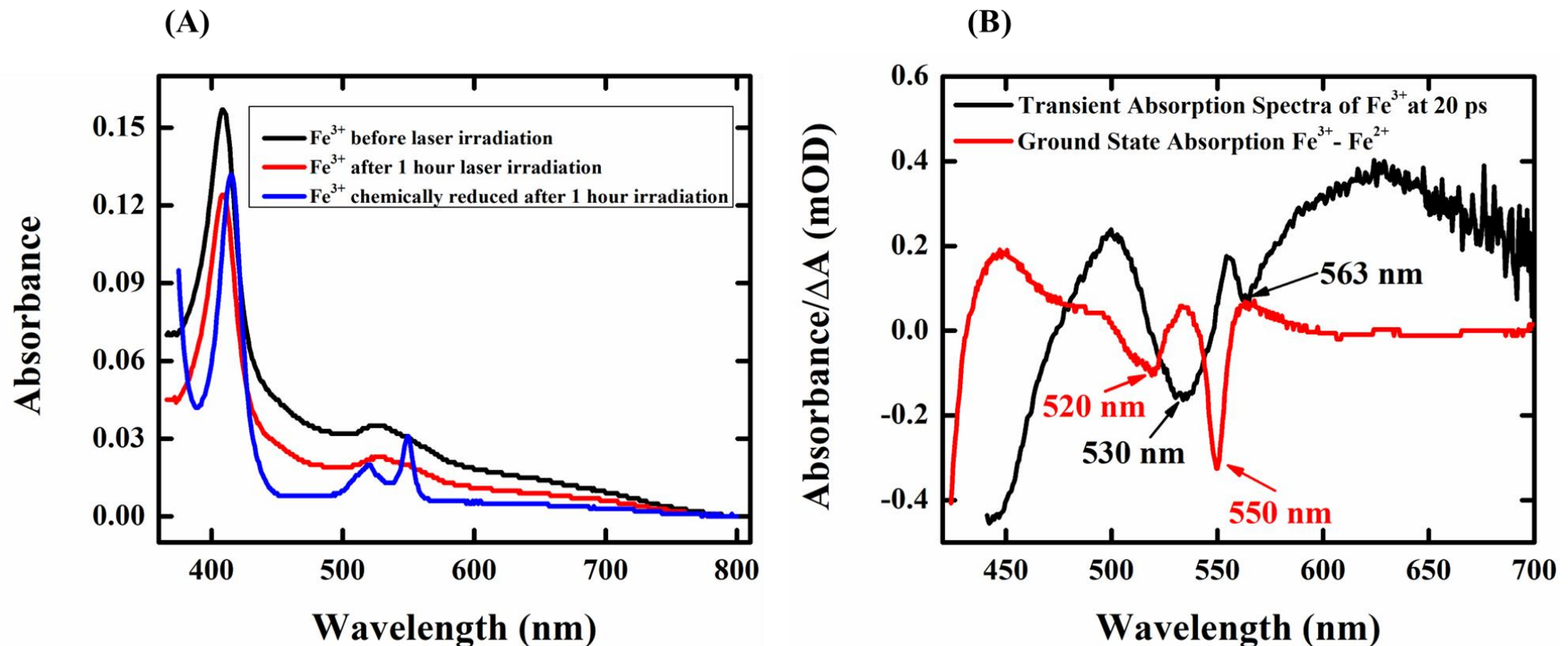


Figure S16 – Comparison of (A) ground state absorption spectra of ferric Cyt *c* in buffer before and after exposure to pump laser and its chemically reduced form after 1 hour of laser exposure, (B) Transient absorption spectra of the ferric form at a later time delay of 20 ps with the difference in the ground state absorption spectra of both ferric and ferrous Cyt *c*. Panel B was used to calculate the quantum yield of photoreduction.



$$\Phi_{Photored} = \frac{A_{554}^{Black}}{A_{550}^{Red}} = 0.0012$$

Figure S17 – (A) Comparison of the decay kinetics of ferric Cyt *c* probed at 600 nm in the ambient and aerobic conditions in the presence of buffer and synthetic polymeric crowders (200 g/L) as mentioned.

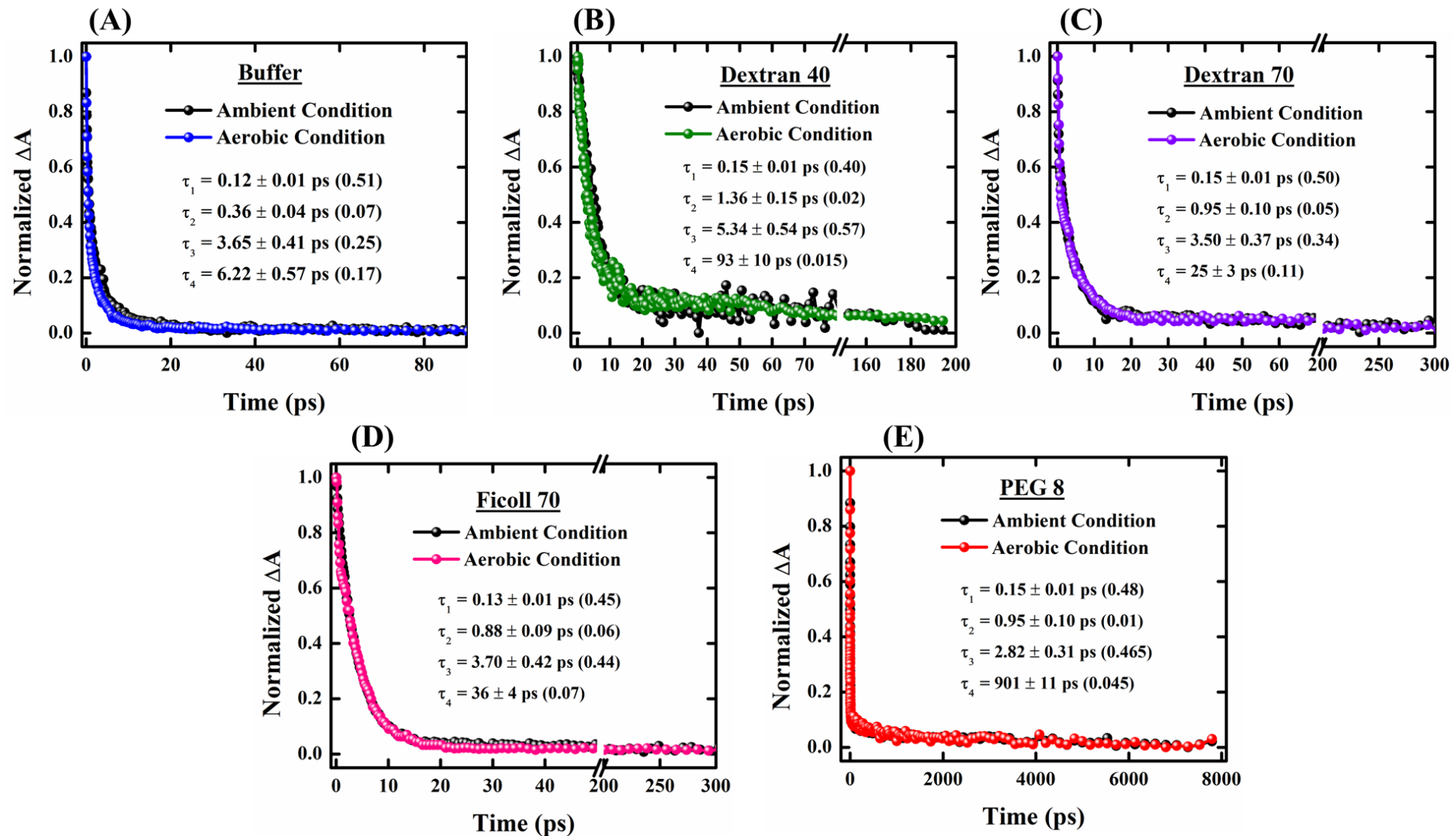
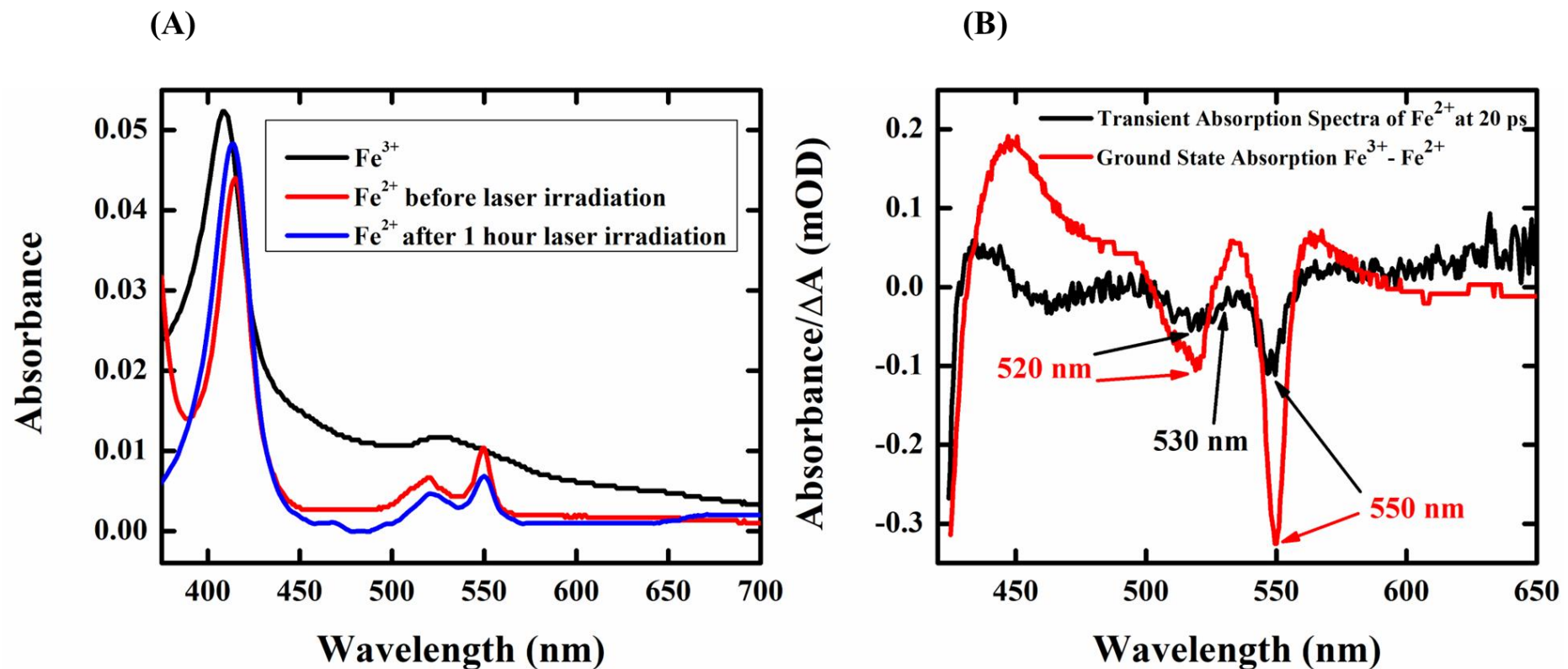


Figure S18– Comparison of (A) ground state absorption spectra of ferrous Cyt *c* in buffer before and after exposure to pump laser and its oxidized form before laser exposure, (B) Transient absorption spectra of the ferrous form at a later time delay of 20 ps with the difference in the ground state absorption spectra of both ferric and ferrous Cyt *c*. Panel B was used to calculate the quantum yield of photooxidation.



$$\Phi_{Photoox} = \frac{A_{530}^{Black}}{A_{550}^{Red}} = 0.00034$$

Figure S19 – (A) Variation in ground state bleach signal (ΔA at 530 nm) for ferric Cyt *c* in buffer (transient absorption spectra provided as inset) and (B) Transient kinetics probed at 600 nm as a function of increasing pump power.

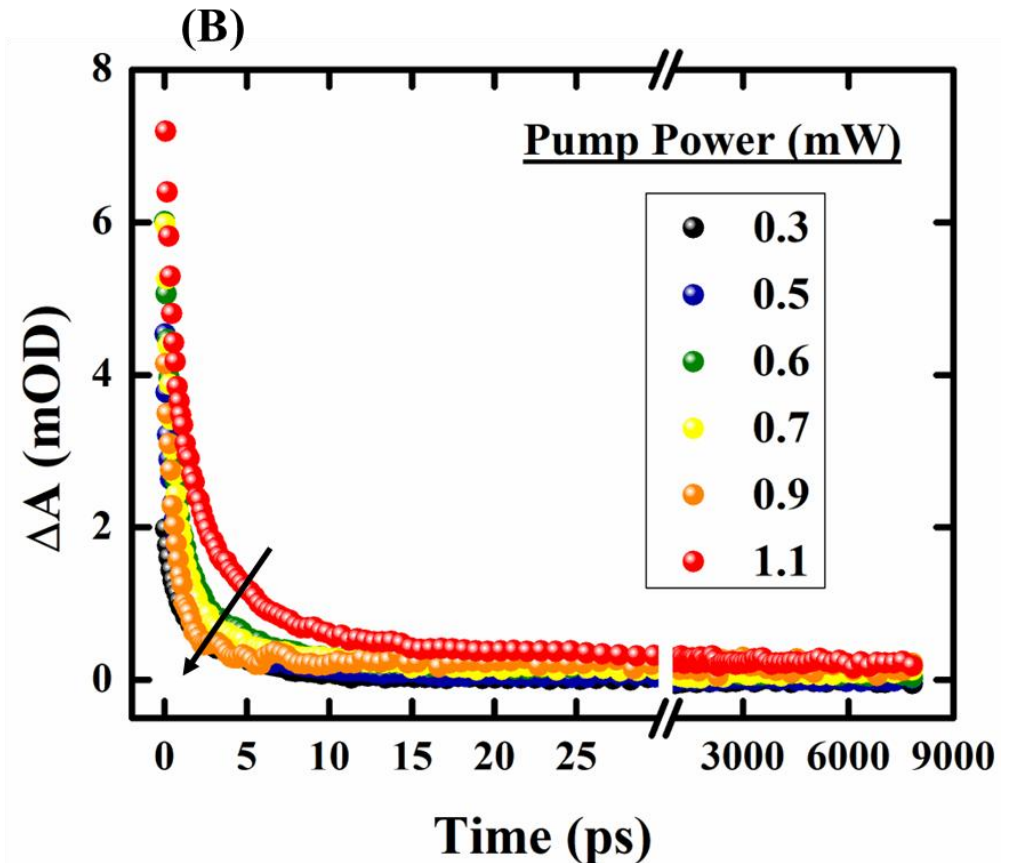
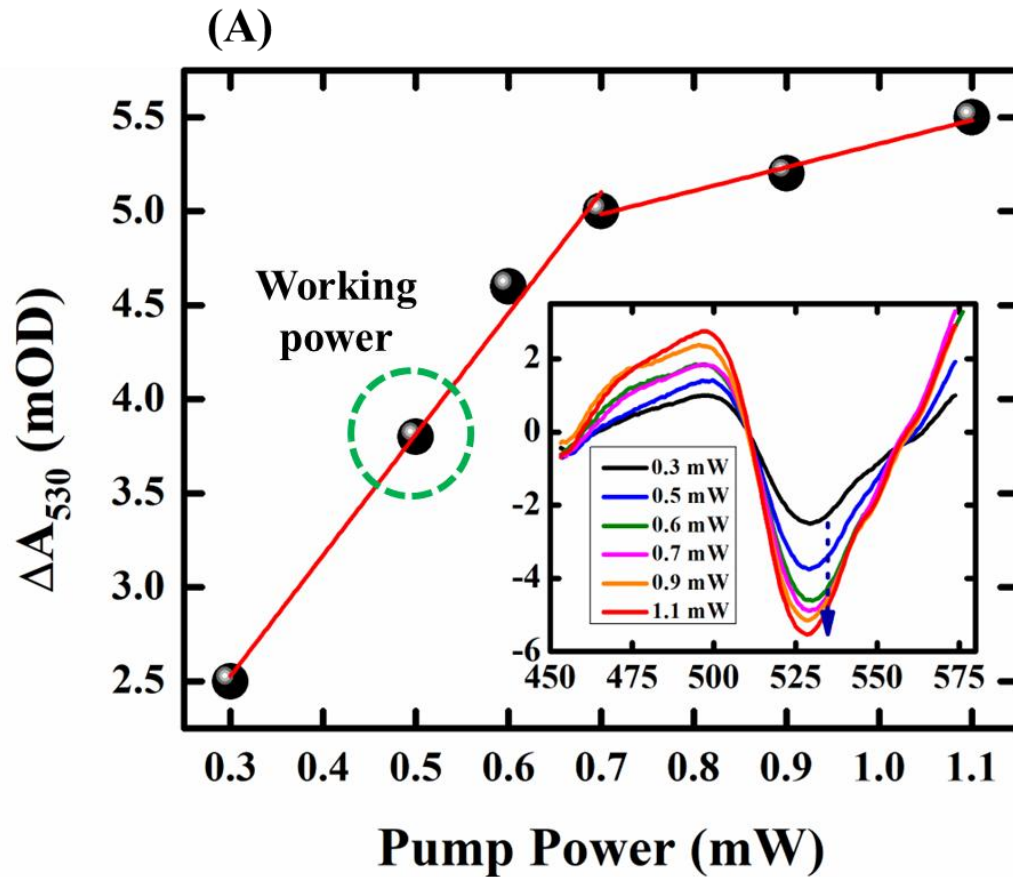


Figure S20 – (A) Variation in ground state bleach signal (ΔA at 550 nm) for ferrous Cyt *c* in buffer (transient absorption spectra provided as inset) and (B) Transient kinetics probed at 575 nm as a function of increasing pump power.

